where n is the number of different species identified, fi is the observed frequency of a particular variant in the quasispecies, and N is the total number of clones analyzed [12,13]. The mean viral complexity in each sample was determined by calculating the total amounts of the Shannon entropy at each nucleotide position divided by the total nucleotide number (e.g., 3215 bases) of each HBV genome sequence.

Nucleotide sequence accession number

All sequence reads have been deposit in DNA Data Bank of Japan Sequence Read Archive (http://www.ddbj.nig.ac.jp/index-e.html) under accession number DRA000435.

Results

Validation of multiplex ultra-deep sequencing of the HBV genome

To differentiate true mutations from sequencing errors in the determined sequences, we first generated viral sequence data from the expression plasmid, pcDNA3-HBV-wt#1, encoding wild-type genotype C HBV genome sequences [28]. For this purpose, we determined the PCR-amplified HBV sequences derived from the expression plasmid using high-fidelity Taq polymerase to take the PCR-induced errors as well as sequencing errors into consideration. Viral sequences determined by the conventional Sanger method were used as reference sequences for aligning the amplicons obtained by ultra-deep sequencing. Three repeated ultra-deep sequencing generated a mean of 77,663 filtered reads, corresponding to a mean coverage of 38,234 fold at each nucleotide site (Table S2). Errors comprised insertions (0.00003%), deletions (0.00135%), and nucleotide mismatches (0.037%). The mean overall error rate was 0.034% (distribution of per-nucleotide error rate ranged from 0 to 0.13%) for the three control experiments, reflecting the error introduced by high-fidelity PCR amplification and by multiplex ultra-deep sequencing that remained after filtering out problematic sequences. We also confirmed that multiplex ultra-deep sequencing with and without the high-fidelity PCR amplification with HBV-specific primer sets showed no significant differences in the error rates on the viral sequence data (mean error rate 0.034% vs 0.043%). Accordingly, we defined the cut-off value in its current platform as 0.3%, a value nearly 1 log above the mean overall error rate.

Next, we performed additional control experiments to verify the detectability of the low abundant mutations that presented at a frequency of less than 0.3%. For this purpose, we introduced expression plasmids with a single-point mutation within that encoding a wild-type viral sequence with a ratio of 1:1000 and assessed the sensitivity and accuracy of quantification using high-fidelity PCR amplification followed by multiplex ultra-deep sequencing in association with the different coverage numbers (Table S3). Repeated control experiments revealed that the threshold for detecting low-abundant mutations at an input ratio of 0.10% among the wild-type sequences ranged between 0.11% and 0.24%, indicating that there was no significant difference in the detection rate or error rates under the different coverage conditions. Based on these results, the accuracy of ultra-deep sequencing in its current platform for detecting low-level viral mutations was considered to be greater than 0.30%.

Viral complexity of the HBV quasispecies in association with clinical status

To clarify HBV quasispecies in association with clinical status, we performed multiplex ultra-deep sequencing and determined the HBV full-genome sequences in the liver and serum with chronic HBV infection. First, we compared the sequences of the viral genome determined in the liver tissue with those in the serum and found no significant differences in the viral population between the liver and serum of the same individual. Indeed, the pattern and distribution of genetic heterogeneity of the viral nucleotide sequences in the liver tissue were similar to those observed in the serum of the same patient (Figure S1), suggesting that a similar pattern of viral heterogeneity was maintained in the liver and serum of patients with chronic HBV infection.

Next, we compared the viral heterogeneity in the liver of chronic-naïve and chronic-NA cases. A mean of 5,962,996 bp nucleotides in chronic-naïve cases and 4,866,783 bp nucleotides in chronic-NA cases were mapped onto the reference sequences, and an overall average coverage depth of 1,855 and 1,514 was achieved for each nucleotide site of the HBV sequences, respectively (Table 2). The frequencies of mutated positions and altered sequence variations detected in each viral genomic region are summarized in Table 2. The overall mutation frequency of the total viral genomic sequences was determined to be 0.87% in chronic-naïve cases and 0.69% in chronic-NA cases. Most genomic changes observed in viral variants were single base substitutions, and the genetic heterogeneity of the viral nucleotide sequences was equally observed throughout the individual viral genetic regions, including the pre-surface (preS), S, pre-core~core (preC-C), and X (Table 2). Consistent with the findings obtained from the viral mutation analyses, the overall viral complexity determined by the Shannon entropy value was 0.047 in chronic-naïve and 0.036 in chronic-NA cases, and the viral complexity was equally observed throughout the individual viral genetic region (Figure 1A). Among chronic-naïve cases, we observed no significant differences in the viral complexity in HBV DNA level, age, or degree of fibrosis (Figure 1B).

High sensitivity of the G1896A pre-C mutant to nucleos(t)ide analogues

Emergence of G1896A mutation in the pre-C region, and A1762T and G1764A mutations in the core-promoter region is well known to be associated with HBe-seroconversion [7–9]. We then evaluated the prevalence of these three mutations in the chronically HBV-infected liver, in association with HBe serologic status and the NA treatment history. In chronic-naive cases, 6 and 8 patients showed the pre- and post- HBeAg seroconversion status, respectively (Table 3). The mean prevalence of the G1896A pre-C mutant in HBeAg-positive cases was lower than that in the HBeAg-negative cases (27.4% and 46.5%, respectively). Importantly, however, 4 of 8 HBeAg-negative cases showed a relatively low prevalence of the G1896A pre-C mutant (Liver #8, #12, #13, #14), and all but one case (Liver #10) showed a high prevalence of the A1762T and G1764A mutations, irrespective of HBe serologic status and NA treatment history (Table 3). These findings suggested that other mutations except G1896A, A1762T and G1764A were also involved in the HBeAg seroconversion status. Notably, liver tissues of all but one (Liver #17) chronic-NA cases showed extremely low levels of the G1896A pre-C mutant (0.0, 0.0, 0.1, and 1.1%), suggesting the high sensitivity of the G1896A pre-C mutant to NA (Table 3).

To confirm the difference of the sensitivity to NA between the wild-type and the G1896A pre-C mutant, we examined the dynamic changes of the relative proportion of the G1896A pre-C mutant in the serum of 14 treatment-naïve patients before and after entecavir administration. Consistent with the findings obtained by ultra-deep sequencing, quantitative real-time PCR revealed that entecavir administration significantly reduced the proportion of the G1896A pre-C mutant in 13 of 14 cases (92.9%) irrespective of their HBeAg serostatus, while the G1896A pre-C mutant were detectable in substantial proportion before treatment in all cases (Figure 2A, 2B and 2C; $p = 0.001$). These results further support the findings that HBV clones comprising the G1896A mutation were more sensitive to NA than those with wild-type sequences.

Prevalence of drug-resistant HBV clones in the liver of treatment-naïve patients

Increasing evidence suggests that drug-resistant viral mutants can be detected in the serum of treatment-naïve patients with chronic HBV infection [20,21]. Thus, we next determined the actual prevalence of spontaneously-developed drug-resistant mutants in chronically-infected liver of treatment-naïve patients to evaluate whether NA treatment potentiates the expansion of drug-resistant clones. The drug-resistant mutations examined included two mutations resistant to lamivudine and entecavir, four mutations resistant to entecavir, and three mutations resistant to adefovir [16,17]. Based on the detection rate of the low-level viral clones determined by the control experiments, we identified the drug-resistant mutants present in each specimen at a frequency of more than 0.3% among the total viral clones. Based on these criteria, at least one resistant mutation was detected in the liver of all of the chronic-naïve cases with chronic HBV infection (Table 4).

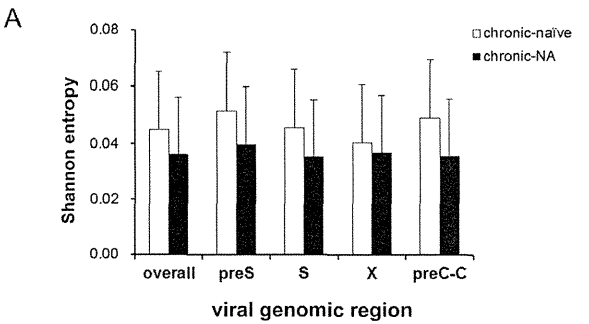

Figure 1. Viral complexity of the HBV quasispecies in association with clinical status. (A) The Shannon entropy values for each viral genomic region were determined in the liver of chronic-naïve and chronic-NA cases. (B) Among the chronic-naïve cases, the Shannon entropy values are shown for patients with serum HBV DNA levels less than 5.0 log copies/ml (<5.0) and greater than 5.0 log copies/ml (≥5.0) (left panel), patients under the age of 55 years (<55) and over the age of 55 (≥55) (middle panel), and patients with low (F1–2) and high (F3–4) liver fibrosis levels (right panel). preS: pre-surface, preC-C: precore~core N.S.: not significant.
doi:10.1371/journal.pone.0035052.g001

Table 2. The frequency of mutation rate and the Shannon entropy in each viral genome region.

	Liver	
	Chronic-naïve (N = 14)	Chronic-NA (N = 5)
Average aligned reads	93,172	76,043
Average aligned nucleotides	5,962,996	4,866,783
Average coverage	1,855	1,514
Mutation rate (%)		
Overall	0.87	0.69
preS	0.92	0.81
S	0.96	0.71
preC-C	1.05	0.72
X	0.63	0.61
Shannon entropy	0.047	0.036

Mutation rate (%): the ratio of total different nucleotides from the reference sequence to total aligned nucleotides.
preS: pre-surface, preC-C: pre-core~core.
doi:10.1371/journal.pone.0035052.t002

Table 3. The prevalence of G1896A mutation in the pre-C region, and A1762T and G1764A mutations in the core-promoter region in the liver of patients chronically infected with HBV.

			Mutation Frequency					
	HBeAg/HBeAb	NA (duration of treatment)	G1896A (Pre C)		A1762T (CP)		G1764A (CP)	
Chronic-naive								
Liver #1	+/−	-	640/1652	(38.7)	1647/1941	(84.9)	1683/1979	(85.0)
Liver #2	+/−	-	9/596	(1.5)	682/687	(99.3)	683/689	(99.1)
Liver #3	+/−	-	273/672	(40.6)	767/769	(99.7)	757/760	(99.6)
Liver #4	+/−	-	204/701	(29.1)	610/625	(97.6)	602/621	(96.9)
Liver #5	+/−	-	27/152	(17.8)	249/250	(99.6)	245/248	(98.8)
Liver #6	+/−	-	228/621	(36.7)	727/729	(99.7)	743/744	(99.9)
Liver #7	−/+	-	740/1193	(62.0)	1908/1913	(99.7)	1888/1913	(98.7)
Liver #8	−/+	-	111/1892	(5.9)	2321/2325	(99.8)	2335/2339	(99.8)
Liver #9	−/+	-	10935/10944	(99.9)	12019/12032	(99.9)	12163/12170	(99.9)
Liver #10	−/+	-	4554/4593	(99.2)	1/5191	(0)	4/5188	(0.1)
Liver #11	−/+	-	811/921	(88.1)	1234/1236	(99.8)	1226/1228	(99.8)
Liver #12	−/+	-	93/1265	(7.4)	1234/1234	(100)	1228/1229	(99.9)
Liver #13	−/+	-	83/877	(9.5)	1465/1529	(95.8)	1485/1549	(95.9)
Liver #14	−/+	-	0/717	(0)	1078/1410	(76.5)	1089/1414	(77.0)
Chronic-NA								
Liver #15	−/+	LAM (156w)	0/390	(0)	441/453	(97.4)	435/448	(97.1)
Liver #16	−/+	ETV (1w)	0/1399	(0)	1624/1632	(99.5)	1625/1630	(99.7)
Liver #17	−/+	LAM (144w)	345/816	(42.3)	988/991	(99.7)	994/994	(100)
Liver #18	−/+	LAM (98w)	2/3963	(0.1)	1015/1188	(85.4)	1190/1194	(99.7)
Liver #19	−/+	LAM (11w)	48/4214	(1.1)	3438/3456	(99.5)	3446/3462	(99.5)

Values in parenthesis show mutation frequency (%): the ratio of total mutant clones to total aligned coverage at each nucleotide sites.
NA: nucleotide analogue, pre C: precore, CP: core promoter, LAM: lamivudine, ETV: entecavir.
doi:10.1371/journal.pone.0035052.t003

The prevalence of the 9 drug-resistant mutations detected by ultra-deep sequencing in 14 chronic-naïve cases ranged from 0.3% to 30.0%, indicating that the proportion of resistant mutations substantially differed in each case. The most commonly detected mutation was M204VI (9 cases) and M250VI (11 cases), which were resistant to lamivudine and entecavir, and entecavir, respectively. Other mutations resistant to adefovir were detected in 7 (50.0%) and 3 (21.4%) cases at A181TV and N236T, respectively (Table 4).

Nine (64.2%) chronic-naïve cases possessed the M204VI mutants in their liver tissues and the proportion of mutant clones among the totally infected viruses ranged from 0.3% to 1.1% among the M204VI mutant-positive patients. In chronic-NA cases, 4 of 5 (80.0%) liver tissues harbored the M204VI mutants with the proportion among the totally infected viruses ranging from 0.4% to 18.7% (Table 4), while the mean serum HBV DNA was suppressed below 2.6 log copies/ml (Table 1). These results suggest that the mutant HBV clones comprising various drug-resistant mutations could latently exist even in the liver of NA treatment-naïve cases.

Expansion of drug-resistant HBV clones harboring M240VI mutations in response to NA administration

To clarify the risk of latent expansion of drug-resistant mutations due to NA treatment, we next examined the early dynamic changes of the prevalence of M204VI mutants in the serum of treatment-naïve patients in response to entecavir treatment. Ultra-deep sequencing provided a mean 40,791- and 38,823-fold coverage of readings, which were mapped to the M204VI nucleotide position at the YMDD sites of each reference sequence in patients before and after entecavir treatment.

Five of 14 (35.7%) patients harbored the M204VI mutations prior to entecavir treatment. Although the serum HBV DNA levels were significantly reduced in response to entecavir in all cases, the M204VI mutant clones were detected in 9 cases (64.3%) after entecavir administration (Table 5). Notably, one patient (Serum #3) who harbored the M240VI mutant clones at baseline had a relatively large expansion of drug-resistant clones among the total viral population in a time-dependent manner in response to entecavir treatment (Table 5). Similarly, M240VI mutant clones became detectable after entecavir administration in four patients (Serum #1, #7, #12, #13) that harbored no resistant mutants at baseline (Table 5). We found no correlation between the degree of the increase in the relative prevalence of M204VI mutant clones and that of the reduction in serum HBV DNA levels. Although only a limited number of patients exhibited a substantial increase in M204VI mutant clones after administration of anti-viral therapy, our findings might suggest that entecavir treatment latently causes selective survival of drug-resistant mutants in treatment naïve patients with chronic HBV infection.

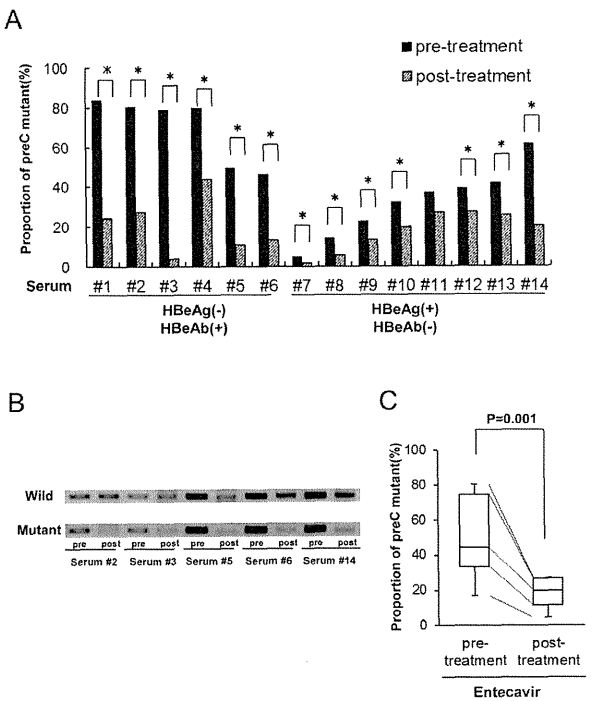

Figure 2. The reduction in the relative proportion of the G1896A pre-C mutant clones after entecavir administration. (A) The relative proportion of the G1896A pre-C mutant was determined in the serum of treatment-naïve patients pre- and post-entecavir administration using quantitative real-time PCR. Serum #1~6 were HBeAg-negative and HBeAb-positive, and Serum #7~14 were HBeAg-positive and HBeAb-negative before treatment. *: $p<0.05$ (B) Semiquantitative PCR analysis was performed using primers specific to the wild-type (upper panel) or G1896A pre-C mutant (lower panel) pre- and post-entecavir administration. A representative result from 5 cases is shown. (C) The relative proportion of the G1896A pre-C mutant was compared in 14 treatment-naïve patients between pre- and post-entecavir administration.
doi:10.1371/journal.pone.0035052.g002

Discussion

Direct population sequencing is the most common method for detecting viral mutations [29]. Conventional sequencing techniques, however, are not efficient for evaluating large amounts of genetic information of the viruses. Newly developed ultra-deep sequencing technology have revolutionized genomic analyses, allowing for studies of the dynamics of viral quasispecies as well as rare genetic variants of the viruses that cannot be detected using standard direct population sequencing techniques [30,31]. The sensitivity of ultra-deep sequencing analysis is primarily limited by errors introduced during PCR amplification and the sequencing reaction, thus it is a challenge to distinguish rare variants from sequencing artifacts. In the present study, we optimized the ultra-deep sequencing with a multiplex-tagging method and reproducibly detected variants within HBV quasispecies that were as rare as 0.3%. Based on this ultra-deep sequencing platform, we determined the abundant genetic heterogeneity of HBV at the intra- and inter-individual levels.

Because of its ability to handle abundant viral genome information, ultra-deep sequencing allowed us to evaluate low-abundant virus variants of patients with chronic HBV infection in detail. It is widely accepted that HBe seroconversion is highly associated with the emergence of G1896A pre-C and/or A1762T and G1764A core promoter mutant clones [7–9]. Unexpectedly, however, our results showed a diverse range of G1896A frequency (0–99.9%) in HBeAg-negative subjects and a high prevalence of core promoter mutations, irrespective of HBe serostatus. Consistent with our observation, previous studies utilizing conventional sequencing methods reported that the frequency of the G1896A pre-C mutant ranged from 12% to 85% [32]. All but one patient (Liver #10) showing a predominance of A1762T and G1764A were infected with genotype C, while patient#10 was infected with genotype B. Because A1762T and G1764A are reported to be significantly more frequent in genotype C [33], the difference in the prevalence of A1762T and G1764A in our study might be a reflection of the viral HBV genotype rather than HBe serostatus. Further investigation of the actual prevalence of these mutations

Table 4. The prevalence of the 9 drug-resistant mutations detected by ultra-deep sequencing derived from liver tissue.

	M204V/I		L180M		T184S/A/I/ L/G/C/M		S202C/G/I		I169T	
Drugs	**LAM/ETV**		**LAM/ETV**		**ETV**		**ETV**		**ETV**	
Chronic-naive										
Liver #1	**27/5421**	**(0.5%)**	2/3694	(-)	9/3886	(-)	5/5613	(-)	5/3784	(-)
Liver #2	**35/5344**	**(0.7%)**	0/538	(-)	1/563	(-)	17/6340	(-)	0/512	(-)
Liver #3	**13/1363**	**(1.0%)**	0/304	(-)	1/358	(-)	1/1379	(-)	0/264	(-)
Liver #4	11/5113	(-)	0/556	(-)	**2/547**	**(0.4%)**	11/5133	(-)	0/639	(-)
Liver #5	**2/117**	**(1.1%)**	0/409	(-)	1/380	(-)	1/189	(-)	1/474	(-)
Liver #6	12/8451	(-)	0/309	(-)	0/328	(-)	22/8457	(-)	0/334	(-)
Liver #7	**10/3098**	**(0.3%)**	1/1547	(-)	3/1477	(-)	8/3161	(-)	0/1621	(-)
Liver #8	**13/2442**	**(0.5%)**	1/2378	(-)	6/2312	(-)	1/2564	(-)	1/2507	(-)
Liver #9	**67/13879**	**(0.5%)**	2/5443	(-)	2/5107	(-)	6/13804	(-)	0/5650	(-)
Liver #10	16/7400	(-)	0/3524	(-)	3/3283	(-)	5/7113	(-)	0/3492	(-)
Liver #11	0/412	(-)	1/1328	(-)	**1/295**	**(0.3%)**	0/425	(-)	3/4729	(-)
Liver #12	**4/1098**	**(0.4%)**	1/1389	(-)	0/1272	(-)	2/1102	(-)	0/1544	(-)
Liver #13	**8/2476**	**(0.3%)**	1/2192	(-)	3/2085	(-)	4/2529	(-)	4/5029	(-)
Liver #14	5/3713	(-)	0/2009	(-)	4/1925	(-)	2/3820	(-)	5/3784	(-)
Chronic-NA										
Liver #15	0/339	(-)	0/49	(-)	0/49	(-)	0/338	(-)	0/40	(-)
Liver #16	**28/7278**	**(0.4%)**	0/4403	(-)	6/4053	(-)	14/7556	(-)	6/6084	(-)
Liver #17	**177/945**	**(18.7%)**	0/1059	(-)	0/1009	(-)	0/945	(-)	0/1051	(-)
Liver #18	**13/2655**	**(0.5%)**	0/1239	(-)	0/1185	(-)	**10/2708**	**(0.4%)**	0/1332	(-)
Liver #19	**80/6795**	**(1.2%)**	0/3168	(-)	2/2971	(-)	3/6734	(-)	0/3384	(-)

	M250V/I		A181T/V		N236T		P237H	
Drugs	**ETV**		**ADV**		**ADV**		**ADV**	
Chronic-naive								
Liver #1	**23/2719**	**(0.9%)**	10/3755	(-)	4/4210	(-)	2/4139	(-)
Liver #2	**9/2079**	**(0.4%)**	**2/549**	**(0.4%)**	1/1144	(-)	1/1188	(-)
Liver #3	**10/1699**	**(0.6%)**	**1/298**	**(0.3%)**	3/1636	(-)	1/1666	(-)
Liver #4	**3/388**	**(0.8%)**	**3/549**	**(0.5%)**	0/560	(-)	0/533	(-)
Liver #5	**2/91**	**(2.2%)**	1/409	(-)	0/55	(-)	0/60	(-)
Liver #6	0/214	(-)	**6/305**	**(2.0%)**	**1/294**	**(0.3%)**	0/257	(-)
Liver #7	**7/1289**	**(0.5%)**	4/1531	(-)	**24/2738**	**(0.9%)**	1/2692	(-)
Liver #8	2/1117	(-)	**689/2336**	**(29.5%)**	2/1713	(-)	0/1639	(-)
Liver #9	**27/7325**	**(0.4%)**	**38/5334**	**(0.7%)**	1/6607	(-)	4/6702	(-)
Liver #10	**12/3815**	**(0.3%)**	0/3454	(-)	**13/3245**	**(0.4%)**	2/3272	(-)
Liver #11	**1/199**	**(0.5%)**	1/972	(-)	0/251	(-)	0/251	(-)
Liver #12	**2/672**	**(0.3%)**	**408/1362**	**(30.0%)**	0/598	(-)	0/597	(-)
Liver #13	1/947	(-)	2/2160	(-)	0/1406	(-)	1/1374	(-)
Liver #14	**23/2719**	**(0.9%)**	10/3755	(-)	4/4210	(-)	2/4139	(-)
Chronic-NA								
Liver #15	**1/303**	**(0.3%)**	**2/49**	**(4.1%)**	0/377	(-)	0/384	(-)
Liver #16	1/922	(-)	0/4403	(-)	1/1597	(-)	3/1572	(-)
Liver #17	0/755	(-)	1/1050	(-)	0/698	(-)	**145/698**	**(20.8%)**
Liver #18	1/1464	(-)	2/1206	(-)	0/3156	(-)	0/3107	(-)
Liver #19	8/3834	(-)	**16/3128**	**(0.5%)**	0/3372	(-)	0/3428	(-)

(-): mutant clones less than 0.3% among total clones at each nucleotide sites.
LAM: lamivudine, ADV: adefovir, ETV: entecavir.
doi:10.1371/journal.pone.0035052.t004

Table 5. The prevalence of M204VI mutation at YMDD site in patients before and after entecavir administration.

	Entecavir treatment				
	Before		**After**		
	Prevalence of the mutated clones		**Prevalence of the mutated clones**		**Period of NA treatment**
Serum #3	222/32,238	(0.7%)	2,284/23,791	(9.6%)	2w
Serum #2	401/34,041	(1.2%)	266/25,301	(1.1%)	24w
Serum #5	521/48,723	(1.1%)	245/25,521	(1.0%)	56w
Serum #8	748/65,573	(1.1%)	336/28,702	(1.2%)	48w
Serum #9	312/30,599	(1.0%)	169/14,172	(1.2%)	56w
Serum #1	9/22,843	(-)	2,839/34,162	(8.3%)	8w
Serum #7	26/65,564	(-)	923/66,458	(1.4%)	4w
Serum #12	91/65,616	(-)	258/27,958	(0.9%)	24w
Serum #13	11/23,209	(-)	206/64,747	(0.3%)	32w
Serum #4	3/7,923	(-)	39/65,575	(-)	12w
Serum #6	52/65,582	(-)	77/55,273	(-)	16w
Serum #10	38/22,522	(-)	8/21,053	(-)	8w
Serum #11	47/43,853	(-)	5/16,520	(-)	16w
Serum #14	42/42,784	(-)	40/36,668	(-)	12w

Mutation frequency (%): the ratio of total mutant clones to total aligned coverage at each nucleotide sites.
(-): mutant clones less than 0.3% among total clones at each nucleotide sites.
doi:10.1371/journal.pone.0035052.t005

and the elucidation of other unknown mutations involved in HBe seroconversion are necessary for a better understanding of the underlying mechanisms of HBe seroconversion.

One thing to be noted is that the majority of the chronic-NA cases had extremely low levels of the G1896A pre-C mutant in their liver tissues, even though those cases were serologically positive for anti-HBe and negative for HBeAg. Moreover, entecavir administration significantly reduced the proportion of the G1896A pre-C mutant in the serum of the majority of patients irrespective of their HBeAg serostatus, while the G1896A pre-C mutant clones were detectable in a substantial proportion before treatment in all cases. These findings suggest that the G1896A pre-C mutant have higher sensitivity to NA than the wild-type viruses. Consistent with this hypothesis, several previous studies reported that NA is effective against acute or fulminant hepatitis caused by possible infection with the G1896A pre-C mutant [34,35]. Based on these findings, early administration of NA might be an effective strategy for treating patients with active hepatitis infected predominantly with the G1896A pre-C mutant.

Ultra-deep sequencing has a relatively higher sensitivity than conventional direct population sequencing and is thus useful for detecting drug-resistant mutations not detected by standard sequencing [20,21]. Recently, we revealed that drug-resistant mutants were widely present in treatment-naïve HCV-infected patients, suggesting a putative risk for the expansion of resistant clones to anti-viral therapy [19]. Here, we demonstrated that various drug-resistant HBV variants are present in a proportion of chronically HBV-infected, NA-naïve patients. Several studies using ultra-deep sequencing provided evidence that naturally-occurring drug-resistant mutations are detectable in treatment-naïve individuals with human immunodeficiency virus-1 infection [30,36,37]. Consistent with the cases of human immunodeficiency virus-1 infection, a few studies detected minor variants resistant to NA in the plasma of treatment-naïve patients with chronic HBV infection [20,21]. It remains unclear, however, whether these minor drug-resistant mutations have clinical significance. Our observation of the relative expansion of viral clones with the M204VI mutation during entecavir therapy in some cases indicates the possibility that preexisting minor mutants might provide resistance against NA through the selection of dominant mutant clones. Future studies with a larger cohort size are required to clarify the clinical implications of the latently existing low-abundant drug-resistant mutations.

The current ultra-deep parallel sequencing technology has limitations in the analyses of viral quasispecies. First, because the massively-parallel ultra-deep sequencing platform is based on a multitude of short reads, it is difficult to evaluate the association between nucleotide sites mapped to different genome regions in a single viral clone. Indeed, potential mutational linkages between the pre-C and reverse transcriptase regions were difficult to elucidate due to the short read length of the shotgun sequencing approach. Second, accurate analysis of highly polymorphic viral clones by ultra-deep sequencing is also difficult because the identification of mutations depends strongly on the mapping to the reference genome sequences.

In conclusion, we demonstrated that the majority of patients positive for anti-HBe and negative for HBeAg lacked the predominant infection of the G1896A pre-C mutant in the presence of NA treatment, suggesting that the G1896A pre-C mutant have increased sensitivity to NA therapy compared with wild-type HBV. We also revealed that drug-resistant mutants are widely present, even in the liver of treatment-naïve HBV-infected patients, suggesting that the preexisting low-abundant mutant clones might provide the opportunity to develop drug resistance against NA through the selection of dominant mutations. Further analyses utilizing both novel and conventional sequencing technologies are necessary to understand the significance and clinical relevance of the viral mutations in the pathophysiology of various clinical settings in association with HBV infection.

Supporting Information

Figure S1 Comparison of the viral complexity between the liver and serum of the same individual. Shannon entropy values throughout the whole viral genome of the liver and serum of the representative two cases are shown. (upper two panels, case #11; lower two panels, case #14). preC-C: pre-core~core, preS: pre-surface, P: polymerase.
(TIF)

Table S1 The oligonucleotide primers for amplifying HBV sequences in each clinical specimen.
(DOCX)

Table S2 Error frequency of Ultra-deep sequencing for the expression plasmid encoding wild-type genotype C HBV genome sequences by the three control experiments.
(DOCX)

Table S3 The sensitivity and accuracy of detecting the low abundant minor clones in association with the different coverage numbers.
(DOCX)

Acknowledgments

We thank Prof. G. Tsujimoto, Dr. F. Sato, Dr. Y. Matsumoto, Dr. Y. Endo, Dr. A Takai, Ms. Y. Nakagawa, Ms. K. Fujii and Ms. C. Hirano for ultra-deep sequencing analysis.

Author Contributions

Conceived and designed the experiments: NN HM. Performed the experiments: NN HM. Analyzed the data: NN HM YU AN TF ST KS TC. Contributed reagents/materials/analysis tools: NN HM YU YO TK SY SU. Wrote the paper: NN HM YU KT TC.

References

1. Dienstag JL (2008) Hepatitis B virus infection. N Engl J Med 359: 1486–1500.
2. Lok AS, McMahon BJ (2007) Chronic hepatitis B. Hepatology 45: 507–539.
3. Chang KM (2010) Hepatitis B immunology for clinicians. Clin Liver Dis 14: 409–424.
4. Murray JM, Purcell RH, Wieland SF (2006) The half-life of hepatitis B virions. Hepatology 44: 1117–1121.
5. Ngui SL, Teo CG (1997) Hepatitis B virus genomic heterogeneity: variation between quasispecies may confound molecular epidemiological analyses of transmission incidents. J Viral Hepat 4: 309–315.
6. Hollinger FB (2007) Hepatitis B virus genetic diversity and its impact on diagnostic assays. J Viral Hepat 14 Suppl 1: 11–15.
7. Akahane Y, Yamanaka T, Suzuki H, Sugai Y, Tsuda F, et al. (1990) Chronic active hepatitis with hepatitis B virus DNA and antibody against e antigen in the serum. Disturbed synthesis and secretion of e antigen from hepatocytes due to a point mutation in the precore region. Gastroenterology 99: 1113–1119.
8. Okamoto H, Yotsumoto S, Akahane Y, Yamanaka T, Miyazaki Y, et al. (1990) Hepatitis B viruses with precore region defects prevail in persistently infected hosts along with seroconversion to the antibody against e antigen. J Virol 64: 1298–1303.
9. Kramvis A, Kew MC (1999) The core promoter of hepatitis B virus. J Viral Hepat 6: 415–427.
10. Carman WF, Fagan EA, Hadziyannis S, Karayiannis P, Tassopoulos NC, et al. (1991) Association of a precore genomic variant of hepatitis B virus with fulminant hepatitis. Hepatology 14: 219–222.
11. Omata M, Ehata T, Yokosuka O, Hosoda K, Ohto M (1991) Mutations in the precore region of hepatitis B virus DNA in patients with fulminant and severe hepatitis. N Engl J Med 324: 1699–1704.
12. Domingo E, Gomez J (2007) Quasispecies and its impact on viral hepatitis. Virus Res. Netherlands. pp 131–150.
13. Fishman SL, Branch AD (2009) The quasispecies nature and biological implications of the hepatitis C virus. Infect Genet Evol 9: 1158–1167.
14. Kwon H, Lok AS (2011) Hepatitis B therapy. Nat Rev Gastroenterol Hepatol.
15. Dienstag JL (2009) Benefits and risks of nucleoside analog therapy for hepatitis B. Hepatology 49: S112–121.
16. Ghany MG, Doo EC (2009) Antiviral resistance and hepatitis B therapy. Hepatology 49: S174–184.
17. Zoulim F, Locarnini S (2009) Hepatitis B virus resistance to nucleos(t)ide analogues. Gastroenterology 137: 1593–1608.e1591–1592.
18. Margulies M, Egholm M, Altman WE, Attiya S, Bader JS, et al. (2005) Genome sequencing in microfabricated high-density picolitre reactors. Nature 437: 376–380.
19. Nasu A, Marusawa H, Ueda Y, Nishijima N, Takahashi K, et al. (2011) Genetic heterogeneity of hepatitis C virus in association with antiviral therapy determined by ultra-deep sequencing. PLoS One 6: e24907.
20. Margeridon-Thermet S, Shulman NS, Ahmed A, Shahriar R, Liu T, et al. (2009) Ultra-deep pyrosequencing of hepatitis B virus quasispecies from nucleoside and nucleotide reverse-transcriptase inhibitor (NRTI)-treated patients and NRTI-naive patients. J Infect Dis 199: 1275–1285.
21. Solmone M, Vincenti D, Prosperi MC, Bruselles A, Ippolito G, et al. (2009) Use of massively parallel ultradeep pyrosequencing to characterize the genetic diversity of hepatitis B virus in drug-resistant and drug-naive patients and to detect minor variants in reverse transcriptase and hepatitis B S antigen. J Virol 83: 1718–1726.
22. Han Y, Huang LH, Liu CM, Yang S, Li J, et al. (2009) Characterization of hepatitis B virus reverse transcriptase sequences in Chinese treatment naive patients. J Gastroenterol Hepatol 24: 1417–1423.
23. Ikeda K, Marusawa H, Osaki Y, Nakamura T, Kitajima N, et al. (2007) Antibody to hepatitis B core antigen and risk for hepatitis C-related hepatocellular carcinoma: a prospective study. Ann Intern Med 146: 649–656.
24. Ruike Y, Imanaka Y, Sato F, Shimizu K, Tsujimoto G (2010) Genome-wide analysis of aberrant methylation in human breast cancer cells using methyl-DNA immunoprecipitation combined with high-throughput sequencing. BMC Genomics 11: 137.
25. Louvel S, Battegay M, Vernazza P, Bregenzer T, Klimkait T, et al. (2008) Detection of drug-resistant HIV minorities in clinical specimens and therapy failure. HIV Med 9: 133–141.
26. Ntziora F, Paraskevis D, Haida C, Magiorkinis E, Manesis E, et al. (2009) Quantitative detection of the M204V hepatitis B virus minor variants by amplification refractory mutation system real-time PCR combined with molecular beacon technology. J Clin Microbiol 47: 2544–2550.
27. Matsumoto Y, Marusawa H, Kinoshita K, Endo Y, Kou T, et al. (2007) Helicobacter pylori infection triggers aberrant expression of activation-induced cytidine deaminase in gastric epithelium. Nat Med 13: 470–476.
28. Marusawa H, Matsuzawa S, Welsh K, Zou H, Armstrong R, et al. (2003) HBXIP functions as a cofactor of survivin in apoptosis suppression. EMBO J 22: 2729–2740.
29. Lok AS, Zoulim F, Locarnini S, Bartholomeusz A, Ghany MG, et al. (2007) Antiviral drug-resistant HBV: standardization of nomenclature and assays and recommendations for management. Hepatology 46: 254–265.
30. Hedskog C, Mild M, Jernberg J, Sherwood E, Bratt G, et al. (2010) Dynamics of HIV-1 quasispecies during antiviral treatment dissected using ultra-deep pyrosequencing. PLoS One 5: e11345.
31. Rozera G, Abbate I, Bruselles A, Vlassi C, D'Offizi G, et al. (2009) Massively parallel pyrosequencing highlights minority variants in the HIV-1 env quasispecies deriving from lymphomonocyte sub-populations. Retrovirology 6: 15.
32. Chowdhury A, Santra A, Chakravorty R, Banerji A, Pal S, et al. (2005) Community-based epidemiology of hepatitis B virus infection in West Bengal, India: prevalence of hepatitis B e antigen-negative infection and associated viral variants. J Gastroenterol Hepatol 20: 1712–1720.
33. Orito E, Mizokami M, Sakugawa H, Michitaka K, Ishikawa K, et al. (2001) A case-control study for clinical and molecular biological differences between hepatitis B viruses of genotypes B and C. Japan HBV Genotype Research Group. Hepatology 33: 218–223.
34. Yu JW, Sun LJ, Yan BZ, Kang P, Zhao YH (2011) Lamivudine treatment is associated with improved survival in fulminant hepatitis B. Liver Int 31: 499–506.
35. Lisotti A, Azzaroli F, Buonfiglioli F, Montagnani M, Alessandrelli F, et al. (2008) Lamivudine treatment for severe acute HBV hepatitis. Int J Med Sci 5: 309–312.
36. Simen BB, Simons JF, Hullsiek KH, Novak RM, Macarthur RD, et al. (2009) Low-abundance drug-resistant viral variants in chronically HIV-infected, antiretroviral treatment-naive patients significantly impact treatment outcomes. J Infect Dis 199: 693–701.
37. Lataillade M, Chiarella J, Yang R, Schnittman S, Wirtz V, et al. (2010) Prevalence and clinical significance of HIV drug resistance mutations by ultra-deep sequencing in antiretroviral-naïve subjects in the CASTLE study. PLoS One 5: e10952.

Hepatology Research JSH

Hepatology Research 2013; 43: 67–71 doi: 10.1111/j.1872-034X.2012.01020.x

Original Article

Efficacy and safety of prophylaxis with entecavir and hepatitis B immunoglobulin in preventing hepatitis B recurrence after living-donor liver transplantation

Yoshihide Ueda,[1] Hiroyuki Marusawa,[1] Toshimi Kaido,[2] Yasuhiro Ogura,[2] Kohei Ogawa,[2] Atsushi Yoshizawa,[2] Koichiro Hata,[2] Yasuhiro Fujimoto,[2] Norihiro Nishijima,[1] Tsutomu Chiba[1] and Shinji Uemoto[2]

Departments of [1]Gastroenterology and Hepatology and [2]Surgery, Graduate School of Medicine, Kyoto University, Kyoto, Japan

Aim: Hepatitis B recurrence after liver transplantation can be reduced to less than 10% by combination therapy with lamivudine (LAM) and hepatitis B immunoglobulin (HBIG). The aim of this study was to evaluate the efficacy and safety of prophylaxis with entecavir (ETV), which has higher efficacy and lower resistance rates than LAM, combined with HBIG in preventing hepatitis B recurrence after living-donor liver transplantation (LDLT).

Methods: Twenty-six patients who received ETV plus HBIG (ETV group) after LDLT for hepatitis B virus (HBV)-related end-stage liver disease were analyzed by comparing with 63 control patients who had received LAM plus HBIG (LAM group).

Results: The survival rates of the patients treated with ETV plus HBIG was 73% after both 1 and 3 years, and there was no statistical difference between the patients in the ETV group and LAM group. No HBV recurrence was detected during the median follow-up period of 25.1 months in the ETV group, whereas the HBV recurrence rate was 4% at 3 years and 6% at 5 years in the LAM group. No patients had adverse effects related to ETV administration.

Conclusion: ETV combined with HBIG provides effective and safe prophylaxis in preventing hepatitis B recurrence after LDLT.

Key words: entecavir, hepatitis B, liver transplantation, living donor

INTRODUCTION

THE RECURRENCE OF hepatitis B virus (HBV) infection after liver transplantation for HBV-related diseases resulted in poor outcomes before the development of effective prophylaxis with lamivudine (LAM) and hepatitis B immunoglobulin (HBIG). Without the prophylaxis, the majority of patients developed recurrent infections due to HBV in the early phases after liver transplantation, and the recurrence resulted in rapidly progressive liver injury, early graft loss and reduced survival.[1–3] The development of prophylaxis dramatically reduced the post-transplant recurrence of hepatitis B and markedly improved prognosis. The most widely used prophylaxis so far has been a combination therapy of LAM and i.v. HBIG.

In the non-transplant setting, the long-term use of LAM resulted in high rates of emergence of resistance to the drug, with rates ranging 14–32% after 1 year and 60–70% after 5 years of treatment. In most cases, the resistance was the result of selection of LAM-resistant mutations in the YMDD motif of the DNA polymerase domain of HBV.[4] Moreover, the emergence of HBV strains with mutations that allow escape from hepatitis B surface antibody (anti-HBs) recognition has been reported in patients vaccinated for HBV,[5,6] in patients with chronic hepatitis B[7,8] and in liver transplant recipients after HBIG administration.[9–11] Therefore, the emergence of LAM resistance and HBIG resistance might

Correspondence: Dr Yoshihide Ueda, Department of Gastroenterology and Hepatology, Graduate School of Medicine, Kyoto University, 54 Kawahara-cho, Shogoin, Sakyo-ku, Kyoto 606-8507, Japan. Email: yueda@kuhp.kyoto-u.ac.jp

Received 15 February 2012; revision 6 March 2012; accepted 28 March 2012.

increase the risk of recurrence during long-term administration of LAM and HBIG, although the rate of HBV recurrence in liver transplant recipients who received prophylaxis with LAM and HBIG for more than 10 years has not been reported to date. At present, several nucleoside analogs are available for the treatment of chronic hepatitis B[4]. Among them, there is entecavir (ETV), a carbocyclic analogue of 2′-deoxyguanosine, which has been shown to have higher efficacy than LAM in patients with chronic hepatitis B. In addition, ETV has a higher genetic barrier to resistance than LAM. The resistance to ETV requires at least three mutations including rtM204V/I, which causes LAM-resistance, rtL180M, and a mutation at one of the following codons: rtT184, rtS202 or rtM250.[4] Therefore, ETV is now used as a first-line therapy in the treatment of chronic hepatitis B worldwide. Data available in the published work suggest that, in transplant recipients, ETV plus HBIG represents a better prophylaxis protocol than LAM plus HBIG for long-term prevention of HBV recurrence after liver transplantation. However, the efficacy and safety of this treatment is largely unknown.

The aim of this study was to evaluate the efficacy and safety of prophylaxis with ETV and HBIG in preventing hepatitis B recurrence after living-donor liver transplantation (LDLT).

METHODS

Patients

WE RETROSPECTIVELY ANALYZED the medical records of 97 patients who underwent LDLT for HBV-related end-stage liver diseases from September 2002 to December 2010. Of these, eight patients were excluded from our study because they had breakthrough hepatitis due to HBV with LAM-resistant mutations and were prescribed LAM plus adefovir before liver transplantation. Accordingly, 89 patients were enrolled in this study.

Prophylaxis with ETV or LAM combined with HBIG

Lamivudine plus HBIG therapy was given to all recipients with HBV-related end-stage liver diseases from September 2002 to November 2006, as reported previously.[12] From December 2006, we changed the protocol for prophylaxis to ETV plus HBIG. ETV at a dose of 0.5 mg/day or LAM at a dose of 100 mg/day was given before transplantation, usually when the patient was referred to the hospital and scheduled for transplantation. Preoperative ETV or LAM prophylaxis was followed by combination with HBIG after transplantation. The first application of HBIG at a dose of 200 IU/kg body mass was administrated i.v. during the anhepatic phase of LDLT, and repeated every day for the first 5 days post-surgery. HBV serological markers were examined at weekly intervals for the first 2 months after the transplant, then at monthly intervals, and 1000 IU of HBIG was periodically administrated to maintain the serum anti-HBs titers at more than 500 IU/L during the first 6 months and 200 IU/L thereafter throughout the follow-up period.[12]

Immunosuppression

Tacrolimus and low-dose steroid therapy were administrated to induce immunosuppression in most patients.[13] Mycophenolate mofetil was administrated to patients who experienced refractory rejection or required reduction of tacrolimus dose due to adverse events. Patients who received ABO blood-type-incompatible transplants were treated with rituximab, plasma exchange, and hepatic artery or portal vein infusion with prostaglandin E1 and methylprednisolone.[14]

Diagnosis of HBV activation

Activation of HBV was diagnosed when hepatitis B surface antigens (HBsAg) and/or HBV DNA became positive in the serum of the patients. After LDLT, HBsAg, anti-HBs and serum HBV DNA were measured at least at 3 monthly intervals. Serological HBV markers, including HBsAg, anti-HBs, hepatitis B core antibody, hepatitis B e antigen (HBeAg) and antibodies to HBeAg (anti-HBe), were measured by chemiluminescent enzyme immunoassay (Fuji Rebio, Tokyo, Japan). Serum HBV DNA titer was analyzed using a commercial polymerase chain reaction (PCR) assay (Amplicor HBV Monitor; Roche, Branchburg, NJ, USA). LAM-resistant YMDD mutant virus was detected by the PCR enzyme-linked mini-sequence assay.[15]

Statistical analysis

Baseline characteristics are shown in Table 1. For continuous variables, medians and ranges are given, and the significance of the data was analyzed with the Wilcoxon rank sum test. For categorical variables, counts are given, and the data were analyzed with the χ^2-test. Survival rates and the rates of patients who showed HBV activation after LDLT were estimated using the Kaplan–Meier method and compared using log-rank tests. $P < 0.05$ was considered significant.

Table 1 Baseline characteristics of 90 patients

	Entecavir + HBIG ($n = 26$)	Lamivudine + HBIG ($n = 63$)	*P*-value
Age (years)	55 (33–68)	53 (26–64)	0.062†
Men/women	19/7	46/17	0.995‡
Primary disease			0.595‡
Acute liver failure	6 (23%)	9 (14%)	
Liver cirrhosis, HCC$^-$	6 (23%)	20 (32%)	
Liver cirrhosis, HCC$^+$	14 (54%)	34 (54%)	
HBV markers before LDLT			
HBsAg$^+$	24 (92%)	61 (97%)	0.350‡
HBeAg$^+$	6 (23%)	18 (29%)	0.595‡
HBV DNA before LDLT	<2.6 (<2.6–7.6<)	3.7 (<2.6–7.6<)	0.010†
<2.6 log IU/mL	14 (54%)	19 (30%)	0.024‡
Follow-up period (months)	25.1 (0.2–58.6)	70.6 (0.5–109.2)	<0.001†

Qualitative variables are shown in number; and quantitative variables expressed as median (range).
†Wilcoxon rank sum test.
‡χ^2-Test.
HBeAg, hepatitis B e antigen; *HBIG*, hepatitis B immunoglobulin; *HBsAg*, hepatitis B surface antigen; *HBV*, hepatitis B virus; *HCC*, hepatocellular carcinoma; *LDLT*, living-donor liver transplantation.

RESULTS

Patient characteristics

TWENTY-SIX PATIENTS who received ETV plus HBIG (ETV group) after LDLT for HBV-related end-stage liver disease were included in this study. Baseline characteristics of these patients are listed in Table 1 and compared with those of 63 control recipients who received LAM plus HBIG (LAM group) at our institute already present in our database. The two groups of patients did not differ significantly by age, sex, primary diseases or serological markers for HBV before LDLT. Serum HBV DNA levels before LDLT were significantly lower in the ETV group than in the LAM group. Fourteen of 26 patients (54%) showed less than 2.6 log IU/mL of serum HBV DNA in the ETV group. Median follow-up period was 25.1 months (range, 0.2–58.6) in the ETV group, whereas it was 70.6 months (range, 0.5–109.2) in the LAM group.

Efficacy and safety of prophylaxis with ETV plus HBIG

Survival rates of the patients treated with ETV plus HBIG estimated by Kaplan–Meier analysis was 73% at both 1 and 3 years (Fig. 1a). There was no difference between the ETV group and the LAM group, in which survival rates were 81% at 1 year, 78% at 3 years and 73% at

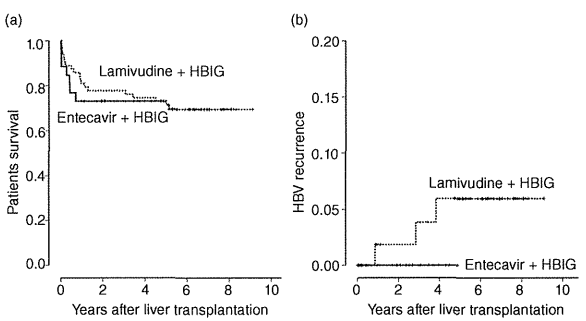

Figure 1 (a) Post-transplantation survival rates and (b) hepatitis B virus (HBV) recurrence after living-donor liver transplantation in HBV positive recipients who received entecavir and hepatitis B immunoglobulin (HBIG) (solid line), or lamivudine and HBIG (dotted line), estimated by Kaplan–Meier method.

5 years. Causes of death in patients in the ETV group were pneumonia ($n = 2$), sepsis ($n = 1$), pulmonary hemorrhage ($n = 1$), cerebral hemorrhage ($n = 1$), graft liver failure ($n = 1$) and multiple organ failure ($n = 1$), none of which were related to ETV. No HBV recurrence was detected in the median follow-up period of 25.1 months in the ETV group, whereas the HBV recurrence rate was 2% at 1 year, 4% at 3 years and 6% at 5 years in the LAM group (Fig. 1b). Three patients in the LAM group had HBV recurrence at 10, 34 and 46 months after LDLT. The emergence of HBV with LAM-resistant mutations in the YMDD motif was confirmed in two of the three patients. HBV mutations of another patient could not be determined because of the low level of serum HBV DNA. As the follow-up period of the ETV group was shorter than that of the LAM group and the HBV recurrence in the LAM group occurred in long-term follow-up after LDLT, the rate of HBV recurrence was not significantly different between the ETV and LAM groups. No patients had adverse events due to ETV administration.

DISCUSSION

IN THIS STUDY, we demonstrated that ETV combined with HBIG provides effective and safe prophylaxis in preventing hepatitis B recurrence after LDLT.

Two studies of patients receiving a combination of ETV and HBIG after liver transplantation have been previously reported.[16,17] One study demonstrated that 30 recipients who received ETV plus HBIG prophylaxis had no recurrence of HBV and no adverse effect relating to ETV.[17] The other study showed that no HBV recurrence was observed in two recipients with HBV-associated cirrhosis receiving ETV, tenofovir and HBIG.[16] Both studies showed the efficacy and safety of prophylaxis with ETV and HBIG in preventing short-term recurrence of HBV after liver transplantation. The current study confirmed their results for longer follow-up periods. Our results showed that prophylaxis with ETV and HBIG has similar efficacy and safety to that with LAM and HBIG, but did not show any further advantage of ETV compared to LAM treatment. Longer follow up might be needed to reveal the difference of HBV recurrence rate. One characteristic of our present report is that all patients in this study underwent LDLT. Our results suggest that prophylaxis with ETV and HBIG in patients after LDLT has similar efficacy and safety to patients after deceased-donor liver transplantation demonstrated in the previous reports.[16,17] More recently, efficacy of ETV monotherapy in preventing recurrence of HBV for liver transplant recipients with chronic hepatitis B was reported.[18] The study demonstrated that most patients showed disappearance of HBsAg and undetectable serum HBV DNA after liver transplantation without HBIG. Although long-term efficacy of ETV monotherapy needs be confirmed, both our data and previous reports suggest that ETV is an effective and safe antiviral agent in the post-transplant setting.

ACKNOWLEDGMENTS

THIS WORK WAS supported by Japan Society for the Promotion of Science (JSPS) Grants-in-Aid for Scientific Research (no. 21229009 and 23590972), Health and Labor Sciences Research Grants for Research on Intractable Diseases, and Research on Hepatitis from the Ministry of Health, Labor and Welfare, Japan, and a grant from Bristol-Myers-Squibb.

REFERENCES

1 Davies SE, Portmann BC, O'Grady JG *et al.* Hepatic histological findings after transplantation for chronic hepatitis B virus infection, including a unique pattern of fibrosing cholestatic hepatitis. *Hepatology* 1991; **13**: 150–7.
2 O'Grady JG, Smith HM, Davies SE *et al.* Hepatitis B virus reinfection after orthotopic liver transplantation. Serological and clinical implications. *J Hepatol* 1992; **14**: 104–11.
3 Todo S, Demetris AJ, Van Thiel D, Teperman L, Fung JJ, Starzl TE. Orthotopic liver transplantation for patients with hepatitis B virus-related liver disease. *Hepatology* 1991; **13**: 619–26.
4 Lok AS, McMahon BJ. Chronic hepatitis B. *Hepatology* 2007; **45**: 507–39.
5 Carman WF, Zanetti AR, Karayiannis P *et al.* Vaccine-induced escape mutant of hepatitis B virus. *Lancet* 1990; **336**: 325–9.
6 Hsu HY, Chang MH, Liaw SH, Ni YH, Chen HL. Changes of hepatitis B surface antigen variants in carrier children before and after universal vaccination in Taiwan. *Hepatology* 1999; **30**: 1312–7.
7 Kohno H, Inoue T, Tsuda F, Okamoto H, Akahane Y. Mutations in the envelope gene of hepatitis B virus variants co-occurring with antibody to surface antigen in sera from patients with chronic hepatitis B. *J Gen Virol* 1996; **77** (Pt 8): 1825–31.
8 Yamamoto K, Horikita M, Tsuda F *et al.* Naturally occurring escape mutants of hepatitis B virus with various mutations in the S gene in carriers seropositive for antibody to hepatitis B surface antigen. *J Virol* 1994; **68**: 2671–6.

9 Carman WF, Trautwein C, van Deursen FJ *et al.* Hepatitis B virus envelope variation after transplantation with and without hepatitis B immune globulin prophylaxis. *Hepatology* 1996; **24**: 489–93.
10 Ghany MG, Ayola B, Villamil FG *et al.* Hepatitis B virus S mutants in liver transplant recipients who were reinfected despite hepatitis B immune globulin prophylaxis. *Hepatology* 1998; **27**: 213–22.
11 Ueda Y, Marusawa H, Egawa H *et al.* De novo activation of HBV with escape mutations from hepatitis B surface antibody after living donor liver transplantation. *Antivir Ther* 2011; **16**: 479–87.
12 Ali H, Egawa H, Uryuhara K *et al.* Prevention of hepatitis B virus recurrence after living donor liver transplantation. *Transplant Proc* 2004; **36**: 2764–7.
13 Ueda Y, Takada Y, Haga H *et al.* Limited benefit of biochemical response to combination therapy for patients with recurrent hepatitis C after living-donor liver transplantation. *Transplantation* 2008; **27** (85): 855–62.
14 Raut V, Mori A, Kaido T *et al.* Splenectomy does not offer immunological benefits in ABO-incompatible liver transplantation with a preoperative rituximab. *Transplantation* 2012; **15** (93): 99–105.
15 Kobayashi S, Shimada K, Suzuki H *et al.* Development of a new method for detecting a mutation in the gene encoding hepatitis B virus reverse transcriptase active site (YMDD motif). *Hepatol Res* 2000; **17**: 31–42.
16 Jimenez-Perez M, Saez-Gomez AB, Mongil Poce L, Lozano-Rey JM, de la Cruz-Lombardo J, Rodrigo-Lopez JM. Efficacy and safety of entecavir and/or tenofovir for prophylaxis and treatment of hepatitis B recurrence post-liver transplant. *Transplant Proc* 2010; **42**: 3167–8.
17 Xi ZF, Xia Q, Zhang JJ *et al.* The role of entecavir in preventing hepatitis B recurrence after liver transplantation. *J Dig Dis* 2009; **10**: 321–7.
18 Fung J, Cheung C, Chan SC *et al.* Entecavir monotherapy is effective in suppressing hepatitis B virus after liver transplantation. *Gastroenterology* 2011; **141**: 1212–9.

PLOS ONE

Comprehensive miRNA Expression Analysis in Peripheral Blood Can Diagnose Liver Disease

Yoshiki Murakami[1]*, Hidenori Toyoda[2], Toshihito Tanahashi[3], Junko Tanaka[4], Takashi Kumada[2], Yusuke Yoshioka[5], Nobuyoshi Kosaka[5], Takahiro Ochiya[5], Y-h Taguchi[6]

1 Department of Hepatology, Graduate School of Medicine, Osaka City University, Osaka, Japan, **2** Department of Gastroenterology, Ogaki Municipal Hospital, Ogaki, Japan, **3** Department of Medical Pharmaceutics, Kobe Pharmaceutical University, Kobe, Japan, **4** Department of Epidemiology, Infectious Disease Control and Prevention, Hiroshima University Graduate School of Biomedical Sciences, Hiroshima, Japan, **5** Division of Molecular and Cellular Medicine, National Cancer Center Research Institute, Tokyo, Japan, **6** Department of Physics, Chuo University, Tokyo, Japan

Abstract

Background: miRNAs circulating in the blood in a cell-free form have been acknowledged for their potential as readily accessible disease markers. Presently, histological examination is the golden standard for diagnosing and grading liver disease, therefore non-invasive options are desirable. Here, we investigated if miRNA expression profile in exosome rich fractionated serum could be useful for determining the disease parameters in patients with chronic hepatitis C (CHC).

Methodology: Exosome rich fractionated RNA was extracted from the serum of 64 CHC and 24 controls with normal liver (NL). Extracted RNA was subjected to miRNA profiling by microarray and real-time qPCR analysis. The miRNA expression profiles from 4 chronic hepatitis B (CHB) and 12 non alcoholic steatohepatitis (NASH) patients were also established. The resulting miRNA expression was compared to the stage or grade of CHC determined by blood examination and histological inspection.

Principal Findings: miRNAs implicated in chronic liver disease and inflammation showed expression profiles that differed from those in NL and varied among the types and grades of liver diseases. Using the expression patterns of nine miRNAs, we classified CHC and NL with 96.59% accuracy. Additionally, we could link miRNA expression pattern with liver fibrosis stage and grade of liver inflammation in CHC. In particular, the miRNA expression pattern for early fibrotic stage differed greatly from that observed in high inflammation grades.

Conclusions: We demonstrated that miRNA expression pattern in exosome rich fractionated serum shows a high potential as a biomarker for diagnosing the grade and stage of liver diseases.

Citation: Murakami Y, Toyoda H, Tanahashi T, Tanaka J, Kumada T, et al. (2012) Comprehensive miRNA Expression Analysis in Peripheral Blood Can Diagnose Liver Disease. PLoS ONE 7(10): e48366. doi:10.1371/journal.pone.0048366

Editor: Xiao-Ping Miao, MOE Key Laboratory of Environment and Health, School of Public Health, Tongji Medical College, Huazhong University of Science and Technology, China

Received May 17, 2012; **Accepted** September 24, 2012; **Published** October 31, 2012

Funding: Y.M, J.T, and T.K. were financially supported by the Ministry of Health, Labour and Welfare of Japan (H22-general-008)and Y.M, J.T, T.K, and Y.T received Grants-in-Aid for scientific research from the Ministry of Education, Culture, Sports, Science and Technology (22590727). The funders had no role in study design, data collection and analysis, decision to publish, or preparation of the manuscript.

Competing Interests: The authors have declared that no competing interests exist.

* E-mail: m2079633@med.osaka-cu.ac.jp

Introduction

MicroRNAs (miRNAs) are a gene family that is evolutionarily conserved and have important roles in the control of many biological processes, such as cellular development, differentiation, proliferation, apoptosis, and metabolism [1]. Aberrant expression of miRNAs in liver tissue has been implicated in the progression of liver fibrosis, and hepatocarcinogenesis [2,3,4]. Recently, two independent groups showed that miR-122 plays a critical role in the maintenance of liver homeostasis and anti-tumor formation [5,6].

Exosome in one of the endoplasmic reticulum carries mRNAs and miRNAs [7]. Recently, it has become clear that exosome perform intercellular signaling through miRNA. miRNAs are released through a ceramide-dependent secretory machinery and are then transferred and become functional in the recipient cells [8]. In a prior study using human blood and cultured cells, several miRNAs were selectively packaged into microvesicle (MV) and actively secreted [9]. In another study, miRNAs originating from EBV was transported by exosome and then participated in the immune response of host cells [10]. In HCC cells as well, this type of exosome-mediated miRNA transfer is an important mechanism of intercellular communication [11].

It has also become clear that exosome can adjust to immune function, control infection or carry the virus itself. Exosomes of T, B and dendritic immune cells contain a repertoire of miRNAs that differ from that of their parent cells [12,13]. Exosomes released from nasopharyngeal carcinoma cells harboring latent EBV were shown to contain LMP1, signal transduction molecules, and virus-encoded miRNAs [14]. Retroviruses evade adaptive immune responses by using nonviral or host exosome biogenesis pathways to form infectious particles and as a mode of infection [15].

Recent evidence has shown that the expression patterns of serum or plasma miRNAs are altered in several diseases, in particular heart disease, sepsis, malignancies, and autoimmune diseases (reviewed in [16]). Discoveries such as this is encouraging and has propelled further research leading to the hypothesis that circulating miRNAs are detectable in serum and plasma in a form sufficiently stable to serve as biomarkers [17,18]. One such example is that tumour-associated miRNAs were found in the serum of diffuse large B-cell lymphoma patients [19]. In other examples, serum levels of miR-34a and miR-122 were associated with histological disease severity in patients with CHC or non-alcoholic fatty-liver disease (NAFLD) [20]. In fact, the serum level of miR-122 strongly correlates with serum ALT activity and with necro-inflammatory activity in patients with CHC and elevated ALT levels. However, there seems to be no significant correlation between fibrosis stage and functional capacity of the liver [21]. The expression levels of miR-122 and miR-194 correlated negatively with age in patients with CHB and HBV associated acute-on-chronic liver failure [22]. The expression level of miR-122 in serum was found to be closely related to non drug-induced acute liver injury [23]. Based on the above, it comes as no surprise that recently, the expression profile from extracellular miRNA is being used clinically to diagnose various diseases.

Here, in order to obtain data with high resolution that is reproducible, we extracted MVs from serum using exoquick and then performed a comprehensive microarray analysis. We attempted to diagnose HCV infection, and ascertain the degree of liver inflammation and fibrosis stage using exosome-rich fractioned miRNA. In short, we investigate if serum-derived miRNAs had the potential to serve as non-invasive bio-markers for various liver diseases.

Results

Reproducible Gene-analysis Using Microarray

In microarray experiments, serum analysis is comparatively easy; however, the downside is that the accuracy and reproducibility of the results are usually not satisfactory. To circumvent this drawback, we devised a procedure that would give us higher accuracy and reproducibility. Serum samples from NL subjects were prepared and divided into two groups; for the first, RNA was extracted using exoquick treated serum, and in the second, RNA was extracted from total serum. Next, miRNA expression was analyzed using Agilent miRNA microarray. The above procedure was performed independently twice (**Fig. 1A**). We compared the miRNA expression pattern among the four microarray results (**Fig. 1B**) and found that miRNA expression analysis using exoquick was the more reliable and reproducible (**Fig. 1C**).

Exosome from normal human prostatic cell lines PNT-2, was yielded by the conventional ultra-centrifugation method [8]. We prepared serums with and without exoquick treatment and performed immunoblot analysis with anti-CD63 (**Fig. 1D**). Bands of the expected relative sizes were detected in serum treated with exoquick. We designated RNA extracted using exoquick treated serum as exosome-rich fractionated RNA.

Unique Expression Pattern of miRNA in CHC

We attempted to diagnose CHC using the miRNA expression pattern found in the peripheral blood samples from 64 CHC and 24 NL. The expression of nine miRNAs (miR-1225-5p, miR-1275, miR-638, miR-762, miR-320c, miR-451, miR-1974, miR-1207-5p, and miR-1246) allowed us to categorize patients as CHC or NL with 96.59% accuracy (**Fig. 2, 3** Table 1 and Table S1). As shown in **Fig. 2C**, CHC and NL were well differentiated due to their distinct miRNA expression patterns. The expression pattern of 12 miRNAs led to the distinction of CHC, CHB, NASH, and NL with 87.50% accuracy (**Fig. 4, S1A,** and Table S1). The accuracy of determining whether samples were CHC or CHB, CHC or NASH, CHB or NASH was 98.35%, 97.37%, and 87.50%, respectively. The accuracy of judging whether samples were NL or CHB, NL or NASH, was 89.29% and 88.89%, respectively (**Fig. 3, S1B** and Table S1). Unlike CHC and NL, there were relatively fewer analyses done of CHB and NASH (due to a small sample size), therefore, we used *"in silico"* resampling to overcome any possible bias. With *"in silico"* we found that it was highly reproducible to determine with high accuracy whether samples were CHC, CHB, NASH, or NL, CHC or CHB, CHC or NASH, CHC or NL, CHB or NASH, CHB or NL, or finally NASH or NL (**Fig. S2 to S8** and Supporting Information).

In order to validate our above-mentioned classifications, we prepared a separate independent sample consisting of 31 CHC, 16 CHB, and 8 NASH. We established miRNA expression patterns using microarray for each of these chronic liver disease groups. We tried to discriminate among the classifications in the independent cohort using the semi-supervised learning method [24] based only on the labels in the original sample group and the selected miRNAs shown in Table S1. The accuracy of judging whether samples were CHB or CHC, CHC or NASH, CHB or NASH, was 74.47%, 87.18%, and 79.19%, respectively (**Fig. S9**, Table 1, and Supporting Information). During the process of obtaining these results, we noticed that different versions of the Feature Extraction (FE) Software provided slightly different results, however it was not possible to fully unify these versions of FE. This may explain the relatively lower performance of the independent group compared with the original samples that mostly used the same FE Software versions.

miRNA Expression Correlates with the Grade of Liver Inflammation

The grade of inflammation for CHC patients was ascertained by liver histological examination, and then samples were divided into four groups A0, A1, A2, and A3 based on their fibrosis stage. miRNA expression profiles were then established for CHC according to each of their inflammation grade. From the four groups (A0 to A3), a combination of six arbitrary pairs is possible. miRNAs which had significant differential expression in five or more of the six pairs were extracted ($p<0.05$). Five miRNAs (miR-1914*, miR-193a-5p, miR-22, miR-659, and miR-711) had expression levels that increased as the severity of liver inflammation progressed. On the other hand, the expression levels of nine miRNAs (miR-1274b, miR-197, miR-1974, miR-21, miR-34a, miR-451, miR-548d-5p, miR-760, and miR-767-3p) significantly decreased with the progression of liver inflammation (**Fig. 5, S10** and Table S2).

The Grade of Liver Fibrosis Corresponded with the Expression Level of miRNAs

As previously noted, CHC samples were divided into F0, F1, F2, and F3 based on patients' fibrotic stage. From these four fibrotic groups, a combination of six arbitrary pairs were possible. miRNAs that had significant differential expression in all six pairs were extracted ($p<0.05$). The expression levels of two miRNAs (miR-483-5p and miR-671-5p) significantly increased the higher the fibrotic stage and the expression level of 14 miRNAs (let-7a, miR-106b, miR-1274a, miR-130b, miR-140-3p, miR-151-3p, miR-181a, miR-19b, miR-21, miR-24, miR-375, miR-548l, miR-93, and miR-941) became progres-

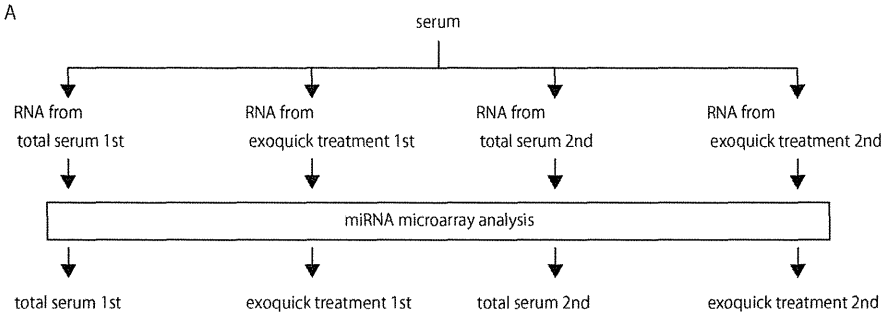

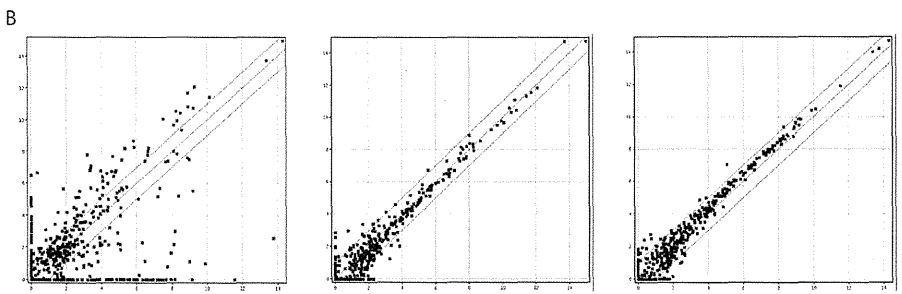

C

	exoquick 1st	total serum 1st	exoquick 2nd	total serum 2nd
exoquick 1st	1	0.836	0.998	0.809
total serum 1st	–	1	0.831	0.930
exoquick 2nd	–	–	1	0.821
total serum 2nd	–	–	–	1

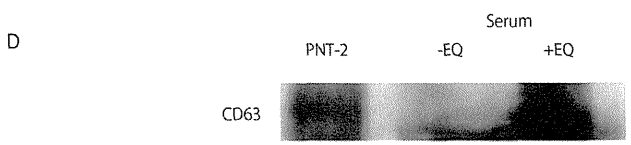

Figure 1. The method used to obtain reproducible data for microarray analysis conducted on serum-extracted samples. A. NL patients' serum were sampled twice. In the first, RNA was extracted first from untreated serum, and then extracted again from serum treated with exoquick. In the second serum sample, RNA was also extracted from both untreated serum and serum treated with exoquick. Microarray analysis was conducted for RNA in a total of four samples. B. Reproducibility test of microarray data. Scatter plots comparing non- normalized signal intensities of miRNAs in two independent experiments from human total serum and exosome rich fraction. Red and black denotes high and low miRNA expressions respectively. Total serum extracted first, versus exosome rich fraction first (left), total serum extracted first versus second (middle), and exosome rich fraction extracted first versus second (right). C. Pearson's pairwise correlations of signal intensities of miRNAs from human total serum and exosome rich fraction. D. Western blot was performed for untreated serum, serum extracted by exoquick and exosome fraction from PNT-2, using anti-CD63.
doi:10.1371/journal.pone.0048366.g001

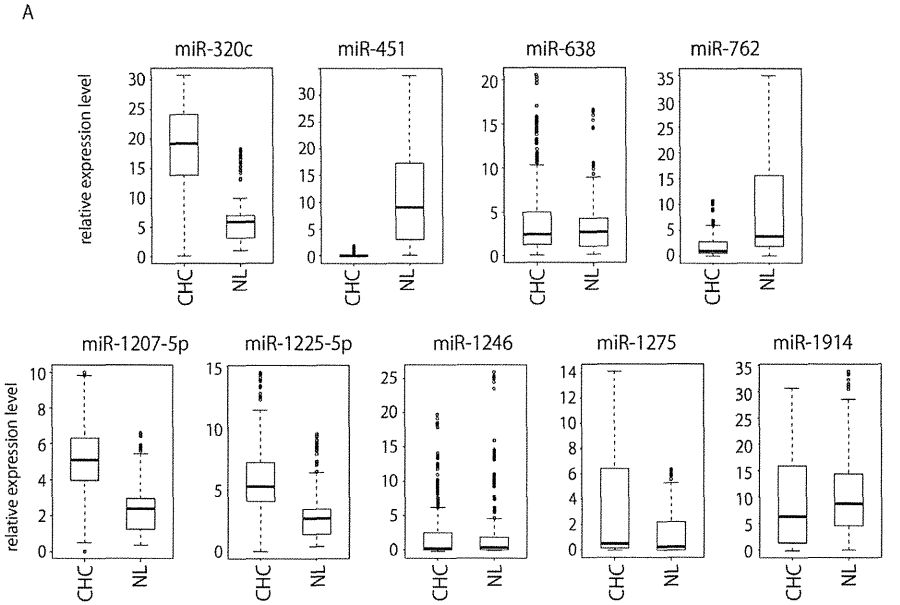

B

		result	
		CHC	NL
prediction	CHC	64	3
	NL	0	21

accuracy 96.6%

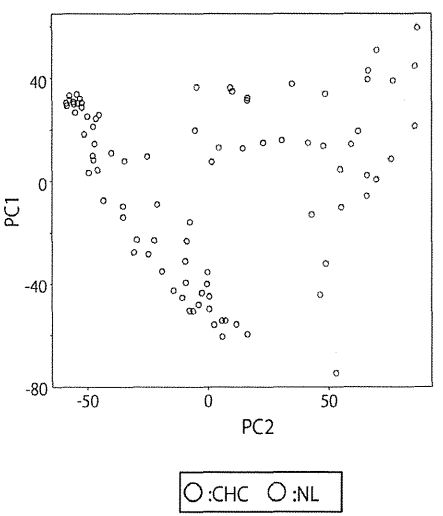

Figure 2. Expression patterns of miRNA used for discriminating between CHC and NL. A. Box plots of expression patterns of the nine miRNAs used for discriminating between CHC and NL. B. Classification of CHC and NL using LOOCV from miRNA expression profile. C. PCA in CHC and NL. The two dimensional embedding of CHC and NL by PCA. The first and second principal component scores computed (not selected for discrimination) of normalized miRNA expression were employed for this plot. Computation was done with ALL.
doi:10.1371/journal.pone.0048366.g002

sively downregulated as liver fibrotic stage increased (**Fig. 6, S11** and Table S2).

Classification of Liver Inflammation Grade and Fibrotic Stage Using miRNA Expression Pattern

We attempted to classify liver inflammation grade and fibrosis stage using miRNA expression pattern. Liver inflammation was diagnosed by Leave One Out Cross-Validation (LOOCV); the accuracy of determining A1 from other inflammation grade was 71.88% and its odds ratio was 7.08. The accuracy of determining A2 and A3 was 75.00% and 82.81%, and their odds ratios were 9.50 and 11.08, respectively. In our study, we were unable to accurately classify A0 because we were limited to only one sample for that grade (**Fig. 7A**). Diagnosis of liver fibrosis by LOOCV showed that determining F0 from the other fibrotic stages had an accuracy of 87.50% and an odds ratio of 14.25. The classification of F1, F2, and F3 had accuracy rates of 65.63%, 70.31%, and 73.44% and odds ratio of 3.16, 6.39 and 5.80, respectively (**Fig. 7B**).

miRNA Expression Level Detected by Real-time qPCR Validated the Microarray Result

Four miRNAs (miR-1207-5p, miR-134, miR-1249, and miR-1183) with expression levels that differed among liver inflammation grades and liver fibrotic stages were chosen in order to confirm the microarray results using stem-loop based real-time qPCR. miRNAs that correlated with other clinical characteristics besides liver fibrosis and inflammation were listed using the Wilcoxon test. We performed two Wilcoxon tests and ranked miRNAs based on their p-value from smallest to largest and selected the miRNAs with the four smallest p-values that were common among the two Wilcoxon tests.

The real-time qPCR result was consistent with the microarray analysis (**Fig. 8**). Here also, we applied *"in silico"* resampling to compensate for the small number of patients used in the real-time qPCR analysis. The results of the *"in silico"* resampling conferred with the results of the real-time qPCR (**Fig. S12**).

miRNA Expression Pattern was Closely Related to Several Clinical Parameters in CHC

Although we observed that miRNA expression correlated with ALT value, we were unable to identify miRNAs that displayed a strong correlation. 12 miRNAs were chosen sequentially from miRNAs with a high absolute correlation coefficient. One to 12 of these selected miRNAs were used to compare the canonical correlation coefficient of the above. When the expression patterns of six of the 12 miRNAs were compared with serum ALT value, the correlation coefficient and p-value were 0.44 and 4.91E−02, respectively. Similarly, when serum Albumin value was compared with the expression pattern of all 12 miRNAs, the correlation coefficient and p-value were 0.59 and 2.04E−02, respectively. Finally when the amount of serum HCVRNA was compared with the expression pattern of 12 miRNAs, the resulting correlation coefficient and p-value were 0.59 and 1.89E−02, respectively (**Fig. 9, S13** and Table S3).

Expression Pattern of a Several miRNAs Correlated to Serum and Hepatic Tissue

In a previous report, we described the miRNA expression pattern found in liver tissues obtained from 105 CHC [2]. From this group, we analyzed the miRNA expression of hepatic tissue and serum in 60 samples. We observed that the expression pattern of three miRNAs (miR-134, miR-200b, miR-324-5p) in hepatic tissue negatively correlated with that in serum, and the expression pattern of miR-370 in hepatic tissue positively correlated with that in serum ($p<0.05$) (Table S4). However, there was no significant correlation between the expression pattern of miR-122 in the hepatic tissue and serum (**Fig. S14** and Table S4).

Discussion

In this comprehensive miRNA analysis in various chronic liver diseases, we observed that aberrant expression of miRNAs was closely related to disease progression. Based on this, we believe that these miRNAs are potential readily accessible biomarkers, useful for diagnosing hepatic viral infection and for grading or staging liver diseases.

Many investigators have elected to use miRNA from serum instead of miRNA from exosome as the candidate for diagnosing diseases [18,20,22,25,26]. In our study, when exoquick was used, exosome could not be isolated therefore other MVs similar in size to exosome were also extracted. In other words, exoquick not only collected miRNAs contained in exosome, but also miRNA that were or were not combined with protein. Despite this, we found that exoquick delivered results that were superior to those obtained without exoquick. Therefore, although the process of analyzing miRNA from serum is simple, we chose to analyze miRNA from exosome rich fraction since it has a higher rate of reproducibility. Moreover, since exosome is closely related to intercellular signaling [14,27], it is expected that data obtained by exosome analysis can clarify the mechanism of chronic infection and inflammation [28].

When we extended our analysis from miR-122 to all miRNAs, it became clear that the expression level of several miRNAs correlated with the progression of liver fibrosis. In fact, recent studies have stated that when the expression levels of adequate numbers of miRNAs is used to identify disease, diagnostic ability is significantly higher than using a single miRNA [29]. In this study, when liver fibrosis was diagnosed using miRNA expression, distinguishing between F0 and F1-3 was done with 87.50% accuracy. Since F0 cannot be distinguished from other stages of chronic liver disease using blood examination, we propose that using miRNA expression pattern may be useful for diagnosing chronic liver disease that is in the early stage.

Previous studies have shown that the level of miR-122 in blood plasma increased earlier than in ALT in the presence of toxic liver injury in rodents [30]. Serum levels of miR-122 in patients with CHC are frequently elevated compared with healthy individuals [21]. Bihrer et al. mentioned that variations in the concentration of miR-122 in serum or plasma tend to be more specific for liver diseases than ALT and AST. This is because miR-122 is almost exclusively expressed in the liver, whereas ALT and AST originate from skeletal muscles and other tissues, therefore their diagnostic value is low [31]. In our study, the expression level of miR-122 had

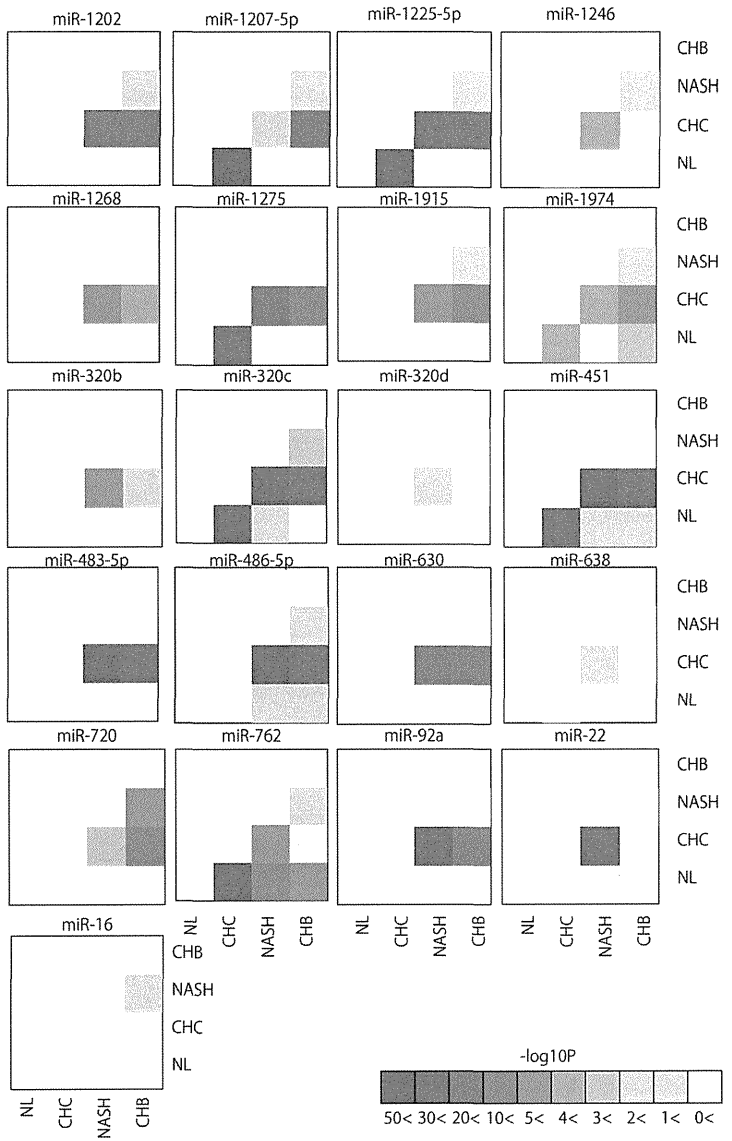

Figure 3. Pairwise heatmap of the miRNAs used for classifying two arbitrary groups. Pairwise heatmap showed the miRNAs and their p-value of two arbitrary groups.
doi:10.1371/journal.pone.0048366.g003

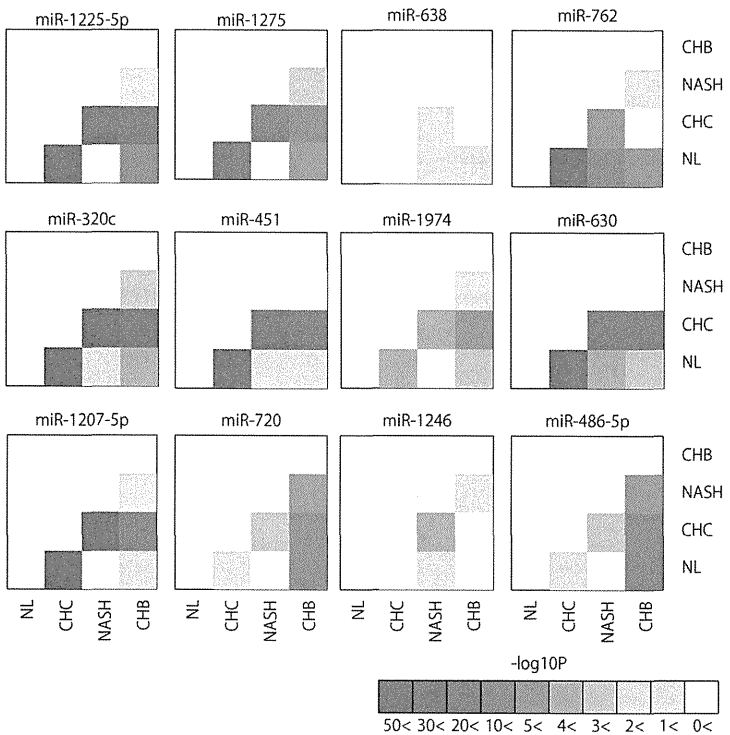

Figure 4. Pairwise heatmap of the miRNAs used for classifying among four groups.
doi:10.1371/journal.pone.0048366.g004

a significant positive correlation with the grade of liver inflammation, serum albumin value, or serum HCVRNA value. However, miR-122 expression did not significantly correlate with liver fibrosis stage. Moreover, there was no correlation between the expression level of miR-122 in liver tissue, and that in serum in the same 60 samples (**Fig. S14**). The expression pattern of only four miRNAs out of total liver tissue miRNAs correlated with the expression patterns of miRNA found in the serum (Table S4). Most serum miRNA had expression patterns that differed from those observed in hepatic tissue samples. Moreover, we observed differences in miRNAs expression between various tissues [32]. These differences were observed even in tissues taken from the same subject; at present we are unclear as to the reason for this phenomenon.

In regards to the progression of liver fibrosis and the expression pattern of miR-21, previous studies concur with our result that miR-21 expression level significantly decreased in response to the progression of liver fibrosis [20]. Taken together, this suggests that any miRNAs that may have been emitted from liver tissue cannot be detected in serum after hepatic cell injury.

The expression pattern of many miRNAs in serum positively correlated with serum ALT, albumin, and HCVRNA levels in this study (**Fig. 9, S13** and Table S3). This result contradicts prior assumptions that no correlation exists between serum miR-122 and HCVRNA serum levels [21]. Three likely reasons for this difference in results are: 1) the detection method used (real-time qPCR versus microarray), 2) the difference in the subjects' ages (the subjects in this study were older), and 3) the difference in the amount of miRNAs (multiple miRNAs vs. a single miRNA) used to identify the clinical parameters of the disease.

CHC and NL were classified with a high level of accuracy using the expression pattern of miRNA. In order to elucidate if the miRNA expression in CHC is common to other chronic liver diseases including CHB, we compared the miRNA expression pattern of CHC with those of NASH and CHB. The result of this analysis was that CHC could be clearly distinguished from both CHB and NASH. These results demonstrate that the varying forms of chronic liver disease have their own unique miRNA expression pattern. NASH is a histological diagnosis that rests on a combination of features and can only be confirmed by liver biopsy. Recently, NASH was diagnosed by first determining the existence of NAFLD from blood samples and then performing an ultrasound tomography. Finally, liver fibrosis stage was determined by Fibroscan

Table 1. Characteristics of subjects in this study of original samples and independent samples.

Original samples

Characteristics	CHC	CHB	NASH	NL
Gender	F: 34/M: 30	F: 2/M: 2	F: 3/M: 9	F:11/M: 13
Age (years)	59.5±8.3	46.8±14.5	52.3±13.1	50.8±12.0
AST (IU/L)	50.1±29.8	83.3±53.7	46.2±16.0	N.D
ALT (IU/L)	57.6±40.6	167.8±170.3	74.5±34.9	N.D
WBC ($x10^3/mm^3$)	5.1±1.5	4.7±1.5	6.2±1.6	N.D
Platelet ($x10^4/mm^3$)	16.6±5.9	14.8±6.3	24.7±8.0	N.D
Total Bilirubin (mg/dl)	0.65±0.22	0.83±0.40	0.76±0.25	N.D
Weight (kg)	57.9±9.18	58.8±4.3	74.9±24.8	59.6±9.6
ALP (IU/L)	267.0±88.4	223.3±25.0	232.7±36.2	N.D
γGTP (IU/L)	46.9±42.3	77.3±82.2	58.4±20.9	N.D
Hemoglobin (g/dl)	13.8±1.2	14.5±0.59	14.7±1.6	N.D
Albumin (g/dl)	4.1±0.4	4.2±0.5	4.4±0.3	N.D

Independent samples

Characteristics	CHC	CHB	NASH
Gender	F: 18/M: 13	F: 10/M: 6	F: 6/M: 2
Age (years)	59.5±8.3	46.8±14.5	54.8±12.7
AST (IU/L)	50.1±29.8	83.3±53.7	80.9±50.0
ALT (IU/L)	57.6±40.6	167.8±170.3	108.9±76.2
WBC ($x10^3/mm^3$)	5.1±1.5	4.7±1.5	5.5±1.8
Platelet ($x10^4/mm^3$)	16.6±5.9	14.8±6.3	19.3±7.6
Total Bilirubin (mg/dl)	0.65±0.22	0.83±0.40	0.73±0.25
Weight (kg)	57.9±9.18	58.8±4.3	66.4±9.9
ALP (IU/L)	267.0±88.4	223.3±25.0	278.6±100.6
γGTP (IU/L)	46.9±42.3	77.3±82.2	130.1±81.23
Hemoglobin (g/dl)	13.8±1.2	14.5±0.59	13.6±1.4
Albumin (g/dl)	4.1±0.4	4.2±0.5	3.8±0.3

Abbreviations; CHC, chronic hepatitis C; CHB, chronic hepatitis B; NASH, non alcoholic steatohepatitis; NL, normal liver (healthy control); N.D, no data.
doi:10.1371/journal.pone.0048366.t001

(reviewed in [33]). However, when the results of these and other measures fail to yield a diagnosis then a pathology evaluation is necessary. Using "*in silico*" resampling to increase the reliability of our data, has led us to believe that NASH diagnosis may be possibly through blood examination.

We tested the reliability of our analysis in two ways and obtained reproducible results in both cases. First we enrolled an independent sample group, and second, we created virtual cohorts using in silico resampling to overcome our small sample size.

In this study we concluded that miRNA profiling is a promising alternative to diagnosing liver disease. This is based on our demonstration that the following evaluations could be performed using suitable miRNA expression profiles (1) determining the stage or grade of chronic liver disease, (2) ascertaining the clinical status of chronic liver diseases, and (3) distinguishing among various forms of chronic liver diseases. While these results suggest there is great potential and benefit of miRNA profiling, future studies in a larger population of CHC patients are warranted to fully elucidate the diagnostic potential of serum miRNA expression.

Materials and Methods

Patient Selection

A cohort of 64 CHC, 4 CHB, and 12 NASH patients who had undergone liver biopsy, as well as 24 healthy control subjects was enrolled. We also prepared independent samples consisting of 31 CHC, 12 CHB, and 8 NASH to validate our results. Patient characteristics are summarized in Table 1 and detailed clinical data is depicted in Table S5. The criteria for exclusion for CHC, CHB, and NASH were: co-infection with human immunodeficiency virus (HIV) types 1 and 2, decompensated liver disease, organ transplantation, immune suppression, autoimmune disorders, consumption of >20 g/day alcohol, and past history of intravenous drug abuse. Healthy controls were selected if they were not infected with HBV, HCV, nor HIV, had normal liver function tests, and had no history of liver disease.

All patients or their guardians provided written informed consent, and Ogaki Municipal Hospital and Kyoto University Graduate School and Faculty of Medicine's Ethics Committee approved all aspects of this study in accordance with the Helsinki Declaration.

Liver Histology and Blood Examination

A liver biopsy specimen was collected from each patient before anti-viral treatment. Histological grading and staging of CHC liver biopsy specimens were performed according to the Metavir classification system [34]. NASH was diagnosed histologically [35].

Serum HCV RNA was quantified before IFN treatment using Amplicor-HCV Monitor Assay (Roche Molecular Diagnostics Co., Tokyo, Japan), while serum HBV DNA was quantified before treatment using Amplicor HBV Monitor Assay (Roche). Pretreatment blood tests were conducted to determine each patient's level of aspartate aminotransferase (AST), alanine aminotransferase (ALT), total bilirubin, alkaline phosphatase, gamma-glutamyl transpeptidase, white blood cell (WBC), platelets, and hemoglobin.

Blood Sampling

Peripheral blood was collected from all subjects directly into serum tubes before anti-viral treatment. The tubes were centrifuged at 1,500 *g* for 10 min at 4°C, sera were aliquoted and additionally centrifuged at 2,000 *g* to completely remove any remaining cells. Sera were stored at −80°C until use.

RNA Preparation

Total RNA from 200 ul of serum was prepared using miRNeasy mini kit (Qiagen, Hilden Germany) according to the manufacturer's instruction. Exosome rich fractionated RNA was prepared using Exoquick (System Biosciences, CA, USA). Briefly, 900 ul of serum was mixed with 250 ul of Exoquick and incubated for 12 hr at 4°C. The tubes were centrifuged at 1500 g for 30 min at room temperature and then supernatant was discarded. The pellet was dissolved with 200 ul of PBS with vigorous vortex. RNA was extracted using miRNeasy mini kit (Qiagen).

Immunoblot Analysis and Exosome Preparation

The procedure for exosome preparation has been previously described [8]. SDS-PAGE gels, SuperSep Ace 5–20% (194–15021) (Wako, Osaka, Japan), were calibrated with Precision Plus Protein Standards (161–0375) (Bio-Rad), and anti-CD63 (1:200)

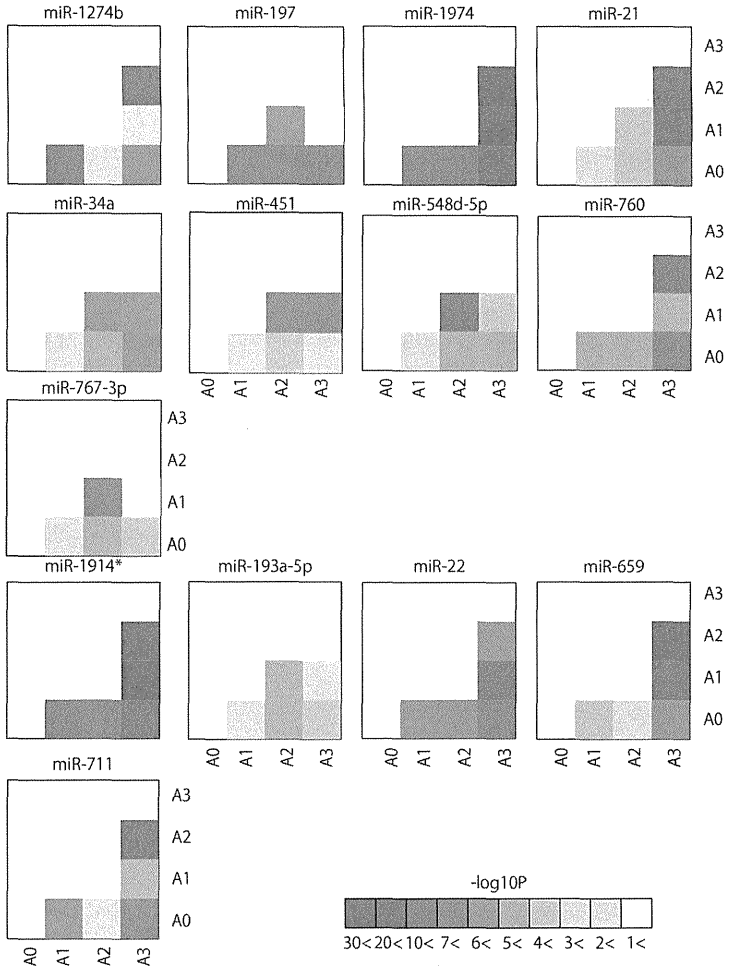

Figure 5. Significantly differentially expressed miRNAs according to liver inflammation grade. Pairwise heatmap showing the miRNAs and p-value of two arbitrary grades.
doi:10.1371/journal.pone.0048366.g005

was used as primary antibodies. The dilution ratio of each antibody is indicated in parentheses. Two secondary antibodies (peroxidase-labeled anti-mouse and anti-rabbit antibodies) were used at a dilution of 1:5000. Bound antibodies were visualized by chemiluminescence using the ImmunoStar LD (Wako) and luminescent images were analyzed by a LuminoImager (LAS-3000; Fuji Film, Inc.). Only gels for CD63 (BD, NJ, USA) detection were run under non-reducing conditions. To exclude the albumin and IgG in serum, Albumin & IgG Depletion SpinTrap kit was used (GE health care, WI, USA). After aliquots isolation, exosome-contained fraction was isolated by Exoquick according to standard instructions.

miRNA Microarray

To detect serum miRNA, 60 ng of RNA was labeled and hybridized using the Human microRNA Microarray Kit (Rel

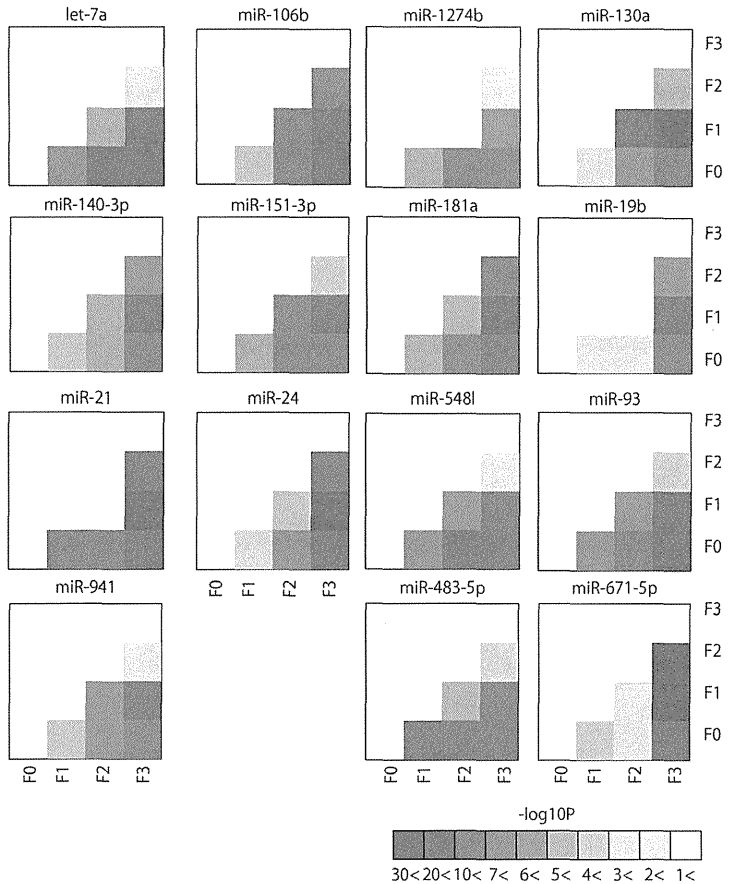

Figure 6. Significantly differentially expressed miRNA according to liver fibrotic stage. Pairwise heatmap showing the miRNAs and p-value of two arbitrary stages.
doi:10.1371/journal.pone.0048366.g006

14.0) (Agilent Technologies, CA, USA) according to the manufacturer's protocol (protocol for use with Agilent microRNA microarrays Version 1.0). Hybridization signals were detected with a DNA microarray scanner G2505B (Agilent Technologies) and the scanned images were analyzed using Agilent feature extraction software (v9.5.3.1). We used raw data (gProcessedSignal) and normalized each expression so as to have zero mean and unit sample variance. The data presented in this manuscript have been deposited in NCBI's Gene Expression Omnibus and are accessible through GEO Series access number GSE33857: http://www.ncbi.nlm.nih.gov/geo/query/acc.cgi?acc = GSE33857.

Real-time qPCR for Human miRNA

To detect miRNA expression level by real-time qPCR, TaqMan® microRNA assay (Applied Biosystems) was used to quantify the relative expression levels of miR-1207-5p (assay ID. 241060), miR-134 (assay ID. 000459), miR-1183 (assay ID. 002841), and miR-1249 (assay ID. 002868). The expression level of miR-16 (assay ID. 000391) was also measured and used as an internal control. cDNA was synthesized using the Taqman miRNA RT Kit (Applied Biosystems). RNA (2 ng/ml) in 5 ml of nuclease free water was added to 3 ml of 5 × RT primer, 10×1.5 µl of reverse transcriptase buffer, 0.15 µl of 100 mM dNTP, 0.19 µl of RNase inhibitor, 4.16 µl of nuclease free water, and 50 U of reverse transcriptase in a total volume of 15 µl. The reaction was performed for 30 min at 16°C, 30 min at 42°C, and 5 min at 85°C.

A

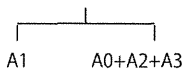

A1 vs A0+A2+A3	
accuracy	71.88%
Fisher's exact test	p-value: 4.07E-04
odds ratio	7.08

		result	
		F	T
prediction	F	22	12
	T	6	24

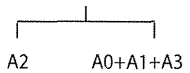

A2 vs A0+A1+A3	
accuracy	75.00%
Fisher's exact test	p-value:2.26E-04
odds ratio	9.50

		result	
		F	T
prediction	F	34	4
	T	12	14

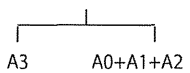

A3 vs A0+A1+A2	
accuracy	82.81%
Fisher's exact test	p-value: 2.30E-03
odds ratio	11.08

		result	
		F	T
prediction	F	47	3
	T	8	6

B

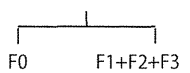

F0 vs F1+F2+F3	
accuracy	87.50%
Fisher's exact test	p-value: 4.95E-02
odds ratio	14.25

		result	
		F	T
prediction	F	54	1
	T	7	2

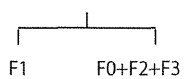

F1 vs F0+F2+F3	
accuracy	64.62%
Fisher's exact test	p-value: 2.73E-02
odds ratio	3.16

		result	
		F	T
prediction	F	21	13
	T	10	20

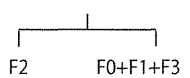

F2 vs F0+F1+F3	
accuracy	70.31%
Fisher's exact test	p-value: 3.24E-03
odds ratio	6.39

		result	
		F	T
prediction	F	33	4
	T	15	12

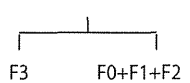

F3 vs F0+F1+F2	
accuracy	73.44%
Fisher's exact test	p-value: 1.35E-02
odds ratio	5.80

		result	
		F	T
prediction	F	39	4
	T	13	8

Figure 7. Determining liver inflammation grade and fibrotic stage using miRNA expression pattern in LOOCV analysis. A. In order to diagnose the grade of liver inflammation, A0 was identified first. Next A1, A2, and A3 were identified in a similar manner as A0. For each, the accuracy rate, P value, and the odds ratio are shown. B. For liver fibrosis stage, F0 was first diagnosed following which the other stages F1, F2, and F3 were diagnosed in a similar manner. For each group the accuracy rate, P value, and the odds ratio are shown.
doi:10.1371/journal.pone.0048366.g007

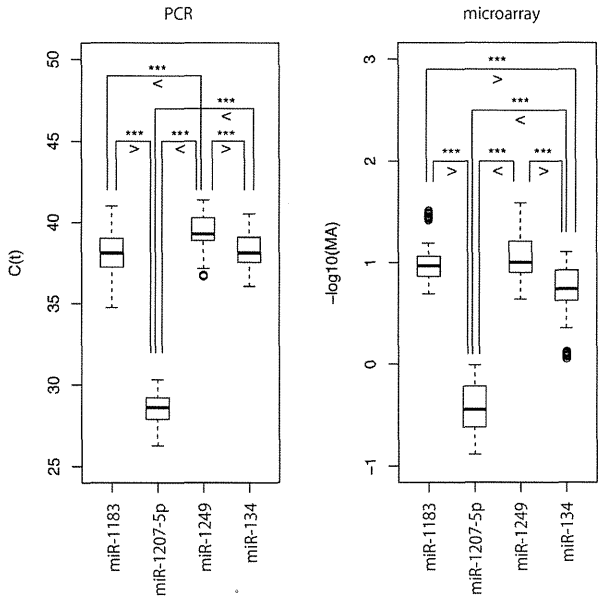

Figure 8. Real-time qPCR validation of microarray analysis. The microarray expression analysis result of four miRNAs was reproduced in real-time PCR analysis. The pairs with $p<0.001$ are marked by "***".
doi:10.1371/journal.pone.0048366.g008

All reactions were run in triplicate. Chromo 4 detector (Bio-rad) was used to detect miRNA expression. To allow for the validation of microarray results with C(t) obtained by qPCR, raw gene expressions were transformed into logarithmic values. P-values were computed via one-sided t test. No averages over probes were taken for the microarray. The above procedures were also done with various packages/functions implemented in R (http://www.r-project.org/).

Statistical Analysis

For symptoms having discrete values, grade pairs were compared with Wilcoxon rank sum test (one-sided); otherwise, P-values were computed from correlation coefficients. In both cases, false discovery rate (FDR) of less then 0.05 computed from the P-value was regarded as significant. Benjamini and Hochberg criterion was used for FDR estimation. All p-values shown are significant even though they are raw numbers. No average over probes was taken before correlation analyses.

The Canonical Correlation Coefficients for miRNA Expression and Clinical Parameters

The canonical correlation coefficients were computed for ALT-miRNA, albumin-miRNA, and HCVRNA-miRNA correlations, using up to 12 miRNA with larger correlation coefficients (see Supporting Information).

Classification Analyses for Liver Fibrosis/inflammation

P-values were computed via one-sided t test using the raw expression values of each miRNA from the samples of CHC and healthy controls. The logarithm of obtained P-values was then transformed into principal components scores via principal components analysis. Following this, grades were discriminated by linear discriminant analysis of CHC ages and the optimal number of principal components.

Selection of miRNAs Required to Diagnose Several Liver Diseases

For specific pairs consisting of one liver disease and a healthy control, their normalized miRNAs expression was transformed into principal components scores via principal components analysis. miRNAs having the larger first and second principal component scores were selected. Following this, the principal component scores of each sample was computed based solely on the selected miRNA expressions. Liver diseases were classified using the optimal number of these principal component scores.

In order to compensate for the relative small number of NASH and CHB patients, we performed "*in silico*" patients resampling analysis of the microarray data (see Supporting Information). All the above procedures were done with various packages/functions implemented in R.

"*In silico*" Resampling

"*In silico*" resampling is a tool often used to overcome the limitation of a small sample size. Using this technique, we combined the clinical traits of existing patients and created various virtual samples. Using these virtual cohorts, we were then able to increase the sample size (see Supporting information).

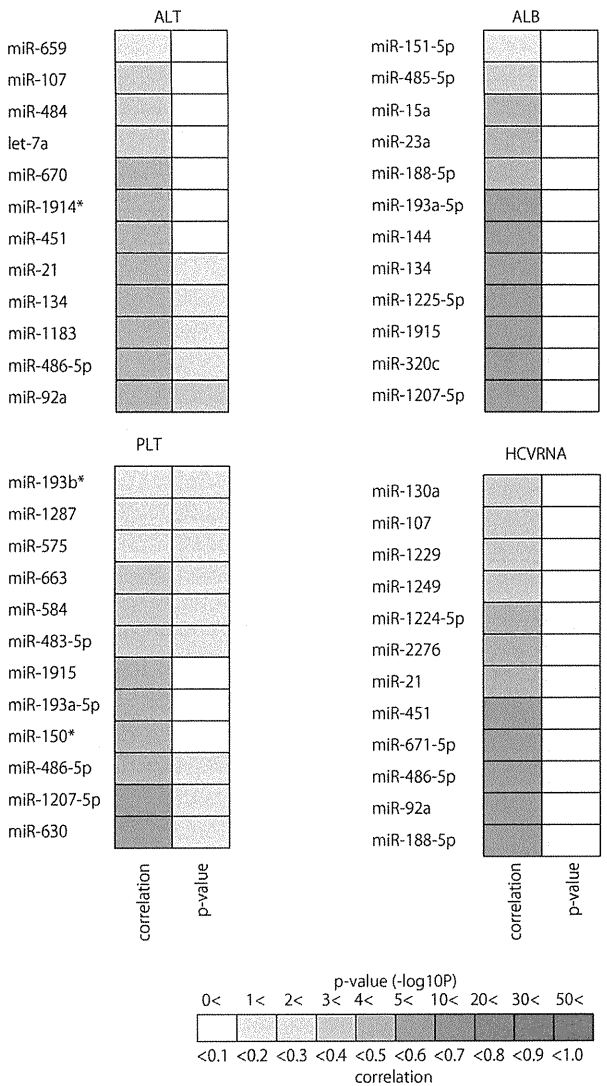

Figure 9. The list of miRNAs used to obtain the maximum correlation coefficient between miRNA expression level, and clinical characteristics. Pairwise heatmap showing miRNAs and their correlation coefficient and p-values.
doi:10.1371/journal.pone.0048366.g009

In order to validate the *"in silico"* resampling results, we prepared another sample set and once again performed *"in silico"* resampling using the microarray data from 99 CHC liver tissue samples [36]. The results proved that "*in silico*" resampling can accurately reproduce an entire population using only a small number of existing samples (see Supporting Information).

Reproducibility Test of Microarray Data

Data were analyzed using the GeneSpring GX10.0.2 (Agilent). Quality control (QC) was applied according to the manufacturer's instructions, and all data were approved by GeneSpring. Following Agilent recommendations, no inter-array normalization was applied because the similarity in miRNA expression among sample arrays was unknown [37]. Scatter plots and Pearson's pairwise correlations were performed with GeneSpring.

Supporting Information

Figure S1 Expression patterns of miRNAs used for discriminating among CHC, NL, CHB, and NASH. Classifying CHC, NL, CHB, and NASH using LOOCV. Distinguishing between two arbitrary groups using LOOCV.
(TIF)

Figure S2 Expression patterns of miRNAs used to discriminate among CHC, CHB, NASH, and NL "in silico" resampling for disease discriminant studies reflected by BMI. A. Box plots of expression pattern of the miRNAs used to discriminate among CHC, CHB, NASH, and NL. B. Discriminating among four groups using LOOCV. Accuracy is 95.25%. C. Two dimensional embedding of CHC, CHB, NASH, and NL by the first and second principle component scores computed with 12 selected miRNAs
(TIF)

Figure S3 The same as Fig.3 for CHC and CHB. A. Box plot of 19 miRNAs used for the discrimination. B. Classification between CHC and CHB. Accuracy is 100%. C. The two dimensional embedding of CHB and CHC by the first and second principal component scores computed with19 selected miRNAs.
(TIF)

Figure S4 The same as Fig.S3 for CHC and NASH. A. Box plots of 20 miRNAs used for the discrimination. B. Classification between CHC and NASH. Accuracy is 100%. C. Two dimensional embedding of CHB and NASH by the first and second principal component scores computed with 19 selected miRNAs
(TIF)

Figure S5 The same as Fig.S3 for CHC and NL. A. Box plots of 9 miRNAs used for the discrimination. B. Classification between CHC and NL. Accuracy is 100%. C. Two dimensional embedding of CHC and NL by the first and second principal component scores computed with 9 selected miRNAs
(TIF)

Figure S6 The same as Fig.S3 for CHB and NL. A. Box plots of 4 miRNAs used for the discrimination. B. Classification between CHB and NL. Accuracy is 93.5%. C. Two dimensional embedding of CHB and NL by the first and second principal component scores computed with 4 selected miRNAs
(TIF)

Figure S7 The same as Fig.S3 for NASH and NL. A. Box plots of 5 miRNAs used for the discrimination. B. Distinguishing between NASH and NL with 84.0% accuracy. C. Two dimensional embedding of NASH and NL by the first and second principal component scores computed with 5 selected miRNAs
(TIF)

Figure S8 The same as Fig.S3 for CHB and NASH pair. A. Box plots of 17 miRNAs used for the discrimination. B. Distinguishing between CHB and NASH with 80.0% accuracy. C. Two dimensional embedding of CHB and NASH by the first and second principal component scores computed with 17 selected miRNAs
(TIF)

Figure S9 Classification of the independent sample using semi-supervised learning based on the labels in the original cohort. A. Classifying CHB and CHC. Accuracy is 74.47%. B. Classifying CHC and NASH. Accuracy is 87.18%. C. Classifying CHB and NASH. Accuracy is 79.19%.
(TIF)

Figure S10 miRNA expression pattern that correlated with the changes in clinical background. miRNAs that were differentially expressed according to the grade of liver inflammation
(TIF)

Figure S11 miRNA expression pattern that correlated with the changes in clinical background. miRNAs that were differentially expressed according to liver fibrosis stage
(TIF)

Figure S12 Real-time qPCR validation of microarray analysis "in silico" resampling for disease discrimination studies reflected by BMI. The result of microarray expression analysis of four miRNAs was reproduced using real-time PCR analysis. Pairs with $p<0.001$ are marked by "***".
(TIF)

Figure S13 The relationship between the expression levels of several miRNAs and serum ALT, albumin, HCVRNA, respectively. Horizontal axis shows the number of miRNAs used in the analysis. Vertical axis shows the correlation index and p-values.
(TIF)

Figure S14 Summary of the relationship between the expression level of miR-122 and several clinical features. A. Expression level of miR-122 positively correlated with an increase in liver inflammatory grade. Asterisk denotes significant differences of $p<0.05$. B. Expression level of miR-122 positively correlated with the serum level of albumin. C. Expression level of miR-122 positively correlated with the amount of serum HCVRNA. D. Expression level of miR-122 in exosome rich fraction did not significantly correlate with that in liver tissues.
(TIF)

Table S1 The list of miRNAs used for classifying arbitrary 2 groups and 4 groups, and their p-values.
(DOCX)

Table S2 Significantly differentially expressed miRNAs according liver inflammation grade and liver fibrotic stage.
(DOCX)

Table S3 The list of miRNAs used to obtain the maximum correlation coefficient between expression level of miRNAs, and clinical characteristics.
(DOCX)

Table S4 List of miRNAs with expression that corresponded in liver tissue and serum.
(DOCX)

Table S5 Clinical background of original samples and independent samples in detail.
(DOCX)

Table S6 Accuracy of LDA for "in silico" resampling.
(DOCX)

Supplemental Information
(DOCX)

References

1. Ambros V (2004) The functions of animal microRNAs. Nature 431: 350–355.
2. Murakami Y, Toyoda H, Tanaka M, Kuroda M, Harada Y, et al. (2011) The progression of liver fibrosis is related with overexpression of the miR-199 and 200 families. PLoS One 6: e16081.
3. Murakami Y, Yasuda T, Saigo K, Urashima T, Toyoda H, et al. (2006) Comprehensive analysis of microRNA expression patterns in hepatocellular carcinoma and non-tumorous tissues. Oncogene 25: 2537–2545.
4. Braconi C, Henry JC, Kogure T, Schmittgen T, Patel T (2011) The role of microRNAs in human liver cancers. Semin Oncol 38: 752–763.
5. Hsu SH, Wang B, Kota J, Yu J, Costinean S, et al. (2012) Essential metabolic, anti-inflammatory, and anti-tumorigenic functions of miR-122 in liver. J Clin Invest 122: 2871–2883.
6. Tsai WC, Hsu SD, Hsu CS, Lai TC, Chen SJ, et al. (2012) MicroRNA-122 plays a critical role in liver homeostasis and hepatocarcinogenesis. J Clin Invest 122: 2884–2897.
7. Valadi H, Ekstrom K, Bossios A, Sjostrand M, Lee JJ, et al. (2007) Exosome-mediated transfer of mRNAs and microRNAs is a novel mechanism of genetic exchange between cells. Nat Cell Biol 9: 654–659.
8. Kosaka N, Iguchi H, Yoshioka Y, Takeshita F, Matsuki Y, et al. (2010) Secretory mechanisms and intercellular transfer of microRNAs in living cells. J Biol Chem 285: 17442–17452.
9. Zhang Y, Liu D, Chen X, Li J, Li L, et al. (2010) Secreted monocytic miR-150 enhances targeted endothelial cell migration. Mol Cell 39: 133–144.
10. Pegtel DM, Cosmopoulos K, Thorley-Lawson DA, van Eijndhoven MA, Hopmans ES, et al. (2010) Functional delivery of viral miRNAs via exosomes. Proc Natl Acad Sci U S A 107: 6328–6333.
11. Kogure T, Lin WL, Yan IK, Braconi C, Patel T (2011) Intercellular nanovesicle-mediated microRNA transfer: a mechanism of environmental modulation of hepatocellular cancer cell growth. Hepatology 54: 1237–1248.
12. Thery C, Ostrowski M, Segura E (2009) Membrane vesicles as conveyors of immune responses. Nat Rev Immunol 9: 581–593.
13. Mittelbrunn M, Gutierrez-Vazquez C, Villarroya-Beltri C, Gonzalez S, Sanchez-Cabo F, et al. (2011) Unidirectional transfer of microRNA-loaded exosomes from T cells to antigen-presenting cells. Nat Commun 2: 282.
14. Meckes DG Jr, Shair KH, Marquitz AR, Kung CP, Edwards RH, et al. (2010) Human tumor virus utilizes exosomes for intercellular communication. Proc Natl Acad Sci U S A 107: 20370–20375.
15. Gould SJ, Booth AM, Hildreth JE (2003) The Trojan exosome hypothesis. Proc Natl Acad Sci U S A 100: 10592–10597.
16. Kosaka N, Iguchi H, Ochiya T (2010) Circulating microRNA in body fluid: a new potential biomarker for cancer diagnosis and prognosis. Cancer Sci 101: 2087–2092.
17. Mitchell PS, Parkin RK, Kroh EM, Fritz BR, Wyman SK, et al. (2008) Circulating microRNAs as stable blood-based markers for cancer detection. Proc Natl Acad Sci U S A 105: 10513–10518.
18. Chen X, Ba Y, Ma L, Cai X, Yin Y, et al. (2008) Characterization of microRNAs in serum: a novel class of biomarkers for diagnosis of cancer and other diseases. Cell Res 18: 997–1006.
19. Lawrie CH (2007) MicroRNAs and haematology: small molecules, big function. Br J Haematol 137: 503–512.
20. Cermelli S, Ruggieri A, Marrero JA, Ioannou GN, Beretta L (2011) Circulating microRNAs in patients with chronic hepatitis C and non-alcoholic fatty liver disease. PLoS One 6: e23937.
21. Bihrer V, Friedrich-Rust M, Kronenberger B, Forestier N, Haupenthal J, et al. (2011) Serum miR-122 as a biomarker of necroinflammation in patients with chronic hepatitis C virus infection. Am J Gastroenterol 106: 1663–1669.
22. Ji F, Yang B, Peng X, Ding H, You H, et al. (2011) Circulating microRNAs in hepatitis B virus-infected patients. J Viral Hepat 18: e242–251.
23. Starkey Lewis PJ, Dear J, Platt V, Simpson KJ, Craig DG, et al. (2011) Circulating microRNAs as potential markers of human drug-induced liver injury. Hepatology 54: 1767–1776.
24. Chapelle O, Scholkopf B, Zien A (2006) Semi-supervised learning. Cambridge, Mass.: MIT Press. x, 508 p. p.
25. Hunter MP, Ismail N, Zhang X, Aguda BD, Lee EJ, et al. (2008) Detection of microRNA expression in human peripheral blood microvesicles. PLoS One 3: e3694.
26. Marquez RT, Bandyopadhyay S, Wendlandt EB, Keck K, Hoffer BA, et al. (2010) Correlation between microRNA expression levels and clinical parameters associated with chronic hepatitis C viral infection in humans. Lab Invest 90: 1727–1736.
27. Mathivanan S, Ji H, Simpson RJ (2010) Exosomes: extracellular organelles important in intercellular communication. J Proteomics 73: 1907–1920.
28. Simons M, Raposo G (2009) Exosomes–vesicular carriers for intercellular communication. Curr Opin Cell Biol 21: 575–581.
29. Keller A, Leidinger P, Bauer A, Elsharawy A, Haas J, et al. (2011) Toward the blood-borne miRNome of human diseases. Nat Methods 8: 841–843.
30. Laterza OF, Lim L, Garrett-Engele PW, Vlasakova K, Muniappa N, et al. (2009) Plasma MicroRNAs as sensitive and specific biomarkers of tissue injury. Clin Chem 55: 1977–1983.
31. Nathwani RA, Pais S, Reynolds TB, Kaplowitz N (2005) Serum alanine aminotransferase in skeletal muscle diseases. Hepatology 41: 380–382.
32. Landgraf P, Rusu M, Sheridan R, Sewer A, Iovino N, et al. (2007) A mammalian microRNA expression atlas based on small RNA library sequencing. Cell 129: 1401–1414.
33. Dowman JK, Tomlinson JW, Newsome PN (2011) Systematic review: the diagnosis and staging of non-alcoholic fatty liver disease and non-alcoholic steatohepatitis. Aliment Pharmacol Ther 33: 525–540.
34. Bedossa P, Poynard T (1996) An algorithm for the grading of activity in chronic hepatitis C. The METAVIR Cooperative Study Group. Hepatology 24: 289–293.
35. Matteoni CA, Younossi ZM, Gramlich T, Boparai N, Liu YC, et al. (1999) Nonalcoholic fatty liver disease: a spectrum of clinical and pathological severity. Gastroenterology 116: 1413–1419.
36. Murakami Y, Tanaka M, Toyoda H, Hayashi K, Kuroda M, et al. (2010) Hepatic microRNA expression is associated with the response to interferon treatment of chronic hepatitis C. BMC Med Genomics 3: 48.
37. Zhang X, Chen J, Radcliffe T, Lebrun DP, Tron VA, et al. (2008) An array-based analysis of microRNA expression comparing matched frozen and formalin-fixed paraffin-embedded human tissue samples. J Mol Diagn 10: 513–519.

Author Contributions

Conceived and designed the experiments: YM NK TO YT. Performed the experiments: YM HT TT YY NK. Analyzed the data: TT YT. Contributed reagents/materials/analysis tools: HT JT TK. Wrote the paper: YM NK TO.

Journal of Medical Virology 84:61–70 (2012)

Predictive Value of Early Viral Dynamics During Peginterferon and Ribavirin Combination Therapy Based on Genetic Polymorphisms Near the *IL28B* Gene in Patients Infected With HCV Genotype 1b

Hidenori Toyoda,[1]* Takashi Kumada,[1] Toshifumi Tada,[1] Kazuhiko Hayashi,[2] Takashi Honda,[2] Yoshiaki Katano,[2] Hidemi Goto,[2] Takahisa Kawaguchi,[3] Yoshiki Murakami,[3] and Fumihiko Matsuda[3]

[1]*Department of Gastroenterology, Ogaki Municipal Hospital, Ogaki, Japan*
[2]*Department of Gastroenterology, Nagoya University Graduate School of Medicine, Nagoya, Japan*
[3]*Center for Genomic Medicine, Kyoto University Graduate School of Medicine, Kyoto, Japan*

A study was carried out to determine whether early viral dynamics retain prediction of the outcome of peginterferon (PEG-IFN) and ribavirin combination therapy based on different genetic polymorphisms near the *IL28B* gene, the strongest baseline predictor of response to this therapy. A total of 272 patients infected with hepatitis C virus (HCV) genotype 1b were grouped according to genetic polymorphisms near the *IL28B* gene (rs8099917). The ability of reduced HCV RNA levels at 4 and 12 weeks after starting therapy to predict a sustained virologic response was evaluated based on these genotypes. Among patients with the TT genotype for rs8099917 (associated with a favorable response), the rates of sustained virologic response were higher in patients with a $\geq$3 $\log_{10}$ reduction in serum HCV RNA levels at 4 weeks after starting therapy ($P < 0.0001$). In contrast, among patients with the TG/GG genotype (associated with an unfavorable response), there were no differences in this rate based on the reduction in HCV RNA levels at 4 weeks. Early viral dynamics at 4 weeks after starting therapy retains its predictive value for sustained virologic response in patients with the TT genotype for rs8099917, but not in patients with the TG/GG genotype. Patients who are likely to achieve sustained virologic response despite unfavorable TG/GG genotype cannot be identified based on early viral dynamics during therapy. In contrast, lack of early virologic response at 12 weeks retains a strong predictive value for the failure of sustained virologic response regardless of *IL28B* polymorphisms, which remains useful as a factor to stop therapy. ***J. Med. Virol. 84:61–70, 2012.*** © 2011 Wiley Periodicals, Inc.

KEY WORDS: chronic hepatitis C; early viral dynamics; genetic polymorphisms near the *IL28B* gene; peginterferon; response-guided therapy; ribavirin

INTRODUCTION

The current standard antiviral therapy for patients with chronic hepatitis C is combination therapy with peginterferon (PEG-IFN) and ribavirin [Ghany et al., 2009]. Although this treatment regimen has increased markedly the number of patients with a sustained virologic response, i.e., the eradication of hepatitis C virus (HCV), only 50% of patients infected with HCV genotype 1 achieved a sustained virologic response approximately.

Many investigators have examined factors that predict the treatment outcome of PEG-IFN and ribavirin combination therapy in patients infected with HCV genotype 1. In addition to the baseline factors, the response of HCV during combination therapy, i.e., the changes in serum HCV RNA levels after starting therapy, has been shown to be an important predictor of the treatment outcome [Zeuzem et al., 2001; Buti

Conflict of interest: None.

*Correspondence to: Hidenori Toyoda, MD, PhD, Department of Gastroenterology, Ogaki Municipal Hospital 4-86, Minaminokawa, Ogaki, Gifu, 503-8502, Japan.
E-mail: hmtoyoda@spice.ocn.ne.jp

Accepted 28 September 2011
DOI 10.1002/jmv.22272
Published online in Wiley Online Library (wileyonlinelibrary.com).

et al., 2002; Berg et al., 2003], with the emphasis on "response-guided therapy" [Lee and Ferenci, 2008; Marcellin and Rizzetto, 2008]. Recent reports have emphasized the importance of evaluating the viral dynamics at 4 weeks after starting therapy to predict a sustained virologic response. A rapid virologic response, in which serum HCV RNA is undetectable at 4 weeks after starting therapy, has been the strongest predictive factor of a sustained virologic response reportedly [Martinez-Bauer et al., 2006; Poordad et al., 2008; de Segadas-Soares et al., 2009; Martinot-Peignoux et al., 2009]. In addition, the predictive value of reduced serum HCV RNA levels at 4 weeks after starting therapy has been clarified further, and a ≥ 3 $\log_{10}$ reduction in HCV RNA levels at 4 weeks after starting therapy has high predictive value that a patient will achieve a sustained virologic response as a final outcome, even in the absence of a rapid virologic response [Toyoda et al., 2011].

In contrast, the lack of an early virologic response, defined as either undetectable serum HCV RNA or HCV RNA levels decreased by >2.0 $\log_{10}$ from the pretreatment level at 12 weeks after starting therapy, has been the most important predictor for the failure of a sustained virologic response in patients infected with HCV genotype 1 reportedly [Fried et al., 2002; Davis et al., 2003]. Therefore, treatment may be discontinued in patients without an early virologic response at 12 weeks of treatment, according to the recommendation in the AASLD guidelines [Ghany et al., 2009].

More recently, several studies reported that genetic polymorphisms near the *IL28B* gene (rs8099917, rs12979860) on chromosome 19 affect the virologic response to PEG-IFN and ribavirin combination therapy in patients infected with HCV genotype 1 [Ge et al., 2009; Suppiah et al., 2009; Tanaka et al., 2009; McCarthy et al., 2010; Rauch et al., 2010]. Furthermore, genetic polymorphisms near the *IL28B* gene are the strongest baseline predictive factor of the final outcome of combination therapy. An additional report showed the effects of genetic polymorphisms near the *IL28B* gene on HCV viral dynamics during PEG-IFN and ribavirin combination therapy [Thompson et al., 2010].

Although early HCV viral dynamics during therapy was shown originally to have a high predictive value for a sustained virologic response in HCV genotype 1-infected patients before genetic polymorphisms near the *IL28B* gene were linked to a therapeutic response, it is not clear whether early viral dynamics retain their predictive value in light of this additional information. The purpose of the present study was to investigate whether response-guided therapy based on viral dynamics at 4 or 12 weeks after initiating therapy retains its ability to predict the final outcome of PEG-IFN and ribavirin combination therapy after accounting for genetic polymorphisms near the *IL28B* gene.

MATERIALS AND METHODS

Patients and Treatment

Between January 2007 and June 2008, a total of 402 patients with chronic hepatitis C received antiviral combination therapy with PEG-IFN and ribavirin for HCV infection at the Ogaki Municipal Hospital or the Nagoya University Hospital. Among these patients, 272 were infected with HCV genotype 1b and had pretreatment HCV RNA levels >5.0 $\log_{10}$ IU/ml based on a quantitative real-time PCR-based method for HCV (HCV COBAS AmpliPrep/COBAS TaqMan System; Roche Molecular Systems, Pleasanton, CA; Lower limit of quantification, 1.7 $\log_{10}$ IU/ml: Lower limit of detection, 1.0 $\log_{10}$ IU/ml) [Colucci et al., 2007; Pittaluga et al., 2008]. This study did not include any patients infected with HCV genotype 1a because this genotype is not found in the general Japanese population.

All patients were given PEG-IFN alpha-2b (Pegintron, Schering-Plough, Tokyo, Japan) weekly and ribavirin (Rebetol, Schering-Plough, Kenilworth, NJ) daily. The PEG-IFN and ribavirin doses were adjusted based on the patient's body weight. Patients weighing $\leq$45 kg were given 60 μg of PEG-IFN alpha-2b once a week, those weighing >45 and $\leq$60 kg were given 80 μg, those weighing >60 and $\leq$75 kg were given 100 μg, those weighing >75 and $\leq$90 kg were given 120 μg, and those weighing >90 kg were given 150 μg. Patients weighing $\leq$60 kg were administered 600 mg of ribavirin per day, those weighing >60 and $\leq$80 kg were given 800 mg per day, and those weighing >80 kg were administered 1000 mg per day. The PEG-IFN and ribavirin doses were modified based on the manufacturer's recommendations. All patients were scheduled to undergo 48 weeks of treatment. The treatment duration was extended up to 72 weeks in some patients. In addition, treatment was discontinued before 48 weeks in some patients who had a low likelihood of achieving an eradication of HCV due to the presence of serum HCV RNA at 24 weeks after starting therapy.

A sustained virologic response was defined as undetectable serum HCV RNA at 24 weeks after ending the therapy. A patient was considered to have relapsed when serum HCV RNA was detectable between the end of treatment and 24 weeks after completing treatment, although serum HCV RNA was undetectable during and at the end of therapy. Patients were considered to have non-response if serum HCV RNA was detectable at 24 weeks after initiating therapy (i.e., null response or partial response according to the American guidelines [Ghany et al., 2009]). Patients were considered to have a rapid virologic response if they had undetectable serum HCV RNA at 4 weeks after starting therapy. An early virologic response was defined as the disappearance or decrease in serum HCV RNA levels by at least 2 $\log_{10}$ at 12 weeks after starting therapy. Patients were considered to have a complete early virologic response if serum HCV RNA was undetectable at 12 weeks after starting therapy and a partial early virologic response if the serum HCV RNA levels had decreased by at least 2 $\log_{10}$ at 12 weeks after initiating therapy. Patients were considered not to have an early virologic response if their HCV RNA levels did not decrease by more than 2 $\log_{10}$ at 12 weeks compared to the pretreatment levels. Patients were considered to have a slow virologic response if the serum HCV RNA became undetectable between 12 and 24 weeks.

The study protocol was in compliance with the Helsinki Declaration and was approved by the ethics committee of the Ogaki Municipal Hospital and the Nagoya University School of Medicine. Prior to initiating the study, each patient provided written informed consent to use the laboratory data, analyze genetic polymorphisms near the *IL28B* gene, and test stored serum samples.

Assessments of Serum HCV RNA Levels and Genetic Polymorphisms Near the *IL28B* Gene

After a patient provided informed consent, serum samples were obtained at the patient's regular hospital visits, just prior to initiating treatment, every 4 weeks during the treatment period, and during the 24-week follow-up period after treatment. Serum samples were stored at −80°C until further use. The HCV RNA levels were measured using a quantitative real-time PCR-based method for HCV (HCV COBAS AmpliPrep/COBAS TaqMan System).

Genotyping of rs 8099917 polymorphisms near the *IL28B* gene was performed using the TaqMan SNP assay (Applied Biosystems, Foster City, California) according to the manufacturer's guidelines. A predesigned and functionally tested probe was used for rs8099917 (C__11710096_10, Applied Biosystems).

Statistical analyses. Quantitative values are reported as the mean ± SD. In between-group differences were analyzed by the chi-square test. Univariate and multivariate analyses using a logistic regression model were performed to identify factors that predict a sustained virologic response, including age, sex, body weight, serum alanine aminotransferase activity, serum aspartate aminotransferase activity, serum gamma-glutamyl transpeptidase levels, serum alkaline phosphatase values, serum albumin levels, total serum bilirubin values, white blood cell counts, hemoglobin, platelet counts, hepatitis activity grade (A0 and A1 vs. A2 and A3), liver fibrosis grade (F0 and F1 vs. F2 and F3), pretreatment HCV RNA levels ($\geq$6.5 $\log_{10}$ vs. <6.5 $\log_{10}$), reduction in peginterferon dose and ribavirin dose, reduction in HCV RNA levels at 4 weeks after starting therapy ($\geq$3 $\log_{10}$ vs. <3 $\log_{10}$), and the type of an early virologic response. All *P*-values are two-tailed, and $P < 0.05$ was considered significant statistically.

RESULTS

The characteristics of the patients examined in this study are shown in Table I. Liver histology was evaluated according to the METAVIR score [The French METAVIR Cooperative Study Group, 1994]. Although some patients had a reduction in their PEG-IFN and ribavirin doses during therapy, respectively, all patients except for those who discontinued the therapy had more than 80% adhesion to both the PEG-IFN and ribavirin regimens. No patients discontinued the therapy because of adverse effects. The treatment duration was extended up to 72 weeks in 51 of 71 patients (71.8%) who exhibited a slow virologic response. As a final outcome, 118 patients (43.4%) achieved a sustained virologic response, 84 patients (30.9%) relapsed, and the remaining 70 patients (25.7%) had no response.

TABLE I. Characteristics of all Study Patients (n = 272)

Age (years)	56.0 ± 10.9
Sex (female/male)	139 (51.1)/133 (48.9)
Body weight (kg)	57.8 ± 10.5
Alanine aminotransferase (IU/L)	64.6 ± 56.4
Aspartate aminotransferase (IU/L)	53.9 ± 42.7
Gamma-glutamyl transpeptidase (IU)	48.5 ± 43.9
Alkaline phosphatase (IU/L)	267.9 ± 101.3
Albumin (g/dl)	4.04 ± 0.37
Total bilirubin (mg/dl)	0.79 ± 0.30
White blood cell count (/μl)	4892 ± 1333
Hemoglobin (g/dl)	14.0 ± 1.3
Platelet count ($\times 10^3/\mu$l)	163 ± 51
Liver histology-activity (A0/A1/A2/A3)*	3 (1.2)/136 (55.3)/ 92 (37.4)/15 (6.1)
Liver histology-fibrosis (F0/F1/F2/F3)*	27 (11.0)/114 (46.3)/ 70 (28.5)/35 (14.2)
Pretreatment HCV RNA concentration ($\log_{10}$ IU/ml)	6.35 ± 0.79
Reduction in the peginterferon dose	81 (29.8)
Reduction in the ribavirin dose	130 (47.8)
Final outcomes (sustained virologic response /relapse/ no response)	118 (43.4)/ 84 (30.9)/70 (25.7)

HCV, hepatitis C virus.
Percentages are shown in parentheses.
*Liver biopsy was not performed in 26 patients.

Reduction in Serum HCV RNA Levels at 4 Weeks after Starting Therapy and Treatment Outcome According to Genetic Polymorphisms Near the *IL28B* Gene

An analysis of genetic polymorphisms at rs8099917 near the *IL28B* gene indicated that 207 patients (76.1%) had a TT genotype, 3 patients had a GG genotype (1.1%), and the remaining 62 patients were TG heterozygote (22.8%). Table II shows the comparison of the background characteristics between patients with the favorable TT genotype and those with the unfavorable TG/GG genotype. As reported previously [Abe et al., 2010], gamma-glutamyl transpeptidase level was higher significantly in patients with the TG/GG genotype. As a final outcome, the rate of a sustained virologic response was higher significantly in patients with the TT genotype. Among 207 patients with the TT genotype, serum HCV RNA became undetectable in 19 patients (9.2%) at 4 weeks after starting therapy (a rapid virologic response). In the remaining 188 patients, the decrease in serum HCV RNA levels at 4 weeks after starting therapy ranged from 0.12

TABLE II. Characteristics of Study Patients According to the Genetic Polymorphisms Near the *IL28B* Gene

	Patients with TT genotype of rs8099917 (n = 207)	Patients with TG/GG genotype of rs8099917 (n = 65)	*P*-value
Age (years)	56.5 ± 10.4	54.4 ± 12.4	0.4112
Sex (female/male)	107 (51.7)/100 (48.3)	32 (49.2)/33 (50.8)	0.8384
Body weight (kg)	57.8 ± 10.9	57.8 ± 9.4	0.8361
Alanine aminotransferase (IU/L)	65.1 ± 53.3	62.8 ± 65.6	0.2548
Aspartate aminotransferase (IU/L)	53.6 ± 34.8	54.7 ± 62.0	0.3339
Gamma-glutamyl transpeptidase (IU)	44.2 ± 37.1	62.3 ± 59.0	0.0003
Alkaline phosphatase (IU/L)	263.1 ± 90.3	282.8 ± 129.9	0.3875
Albumin (g/dl)	4.04 ± 0.36	4.05 ± 0.43	0.8020
Total bilirubin (mg/dl)	0.79 ± 0.30	0.76 ± 0.32	0.3010
White blood cell count (/μl)	4826 ± 1333	5100 ± 1320	0.1608
Hemoglobin (g/dl)	13.9 ± 1.3	14.1 ± 1.4	0.3339
Platelet count ($\times 10^3$/μl)	161 ± 49	169 ± 57	0.3871
Liver histology-activity (A0/A1/A2/A3)*	2 (1.1)/98 (52.4)/ 74 (39.6)/13 (6.9)	1 (1.7)/38 (64.4)/ 18 (30.5)/2 (3.4)	0.3241
Liver histology-fibrosis (F0/F1/F2/F3)*	21 (11.2)/83 (44.4)/ 57 (30.5)/26 (13.9)	6 (10.2)/31 (52.5)/ 13 (22.0)/9 (15.3)	0.6401
Pretreatment HCV RNA concentration ($\log_{10}$ IU/ml)	6.37 ± 0.85	6.29 ± 0.55	0.0582
Reduction in the peginterferon dose	61 (29.5)	20 (30.8)	0.9644
Reduction in the ribavirin dose	101 (48.8)	29 (44.6)	0.5565
Final outcomes (sustained virologic response /relapse/ no response)	106 (51.2)/ 69 (33.3)/32 (15.5)	12 (18.4)/15 (23.1)/ 38 (58.5)	<0.0001

HCV, hepatitis C virus.
Percentages are shown in parentheses.
*Liver biopsy was not performed in 26 patients.

$\log_{10}$ to 5.71 $\log_{10}$ (mean, 3.12 $\log_{10}$). The reduction in serum HCV RNA levels was ≥3 $\log_{10}$ in 98 patients (47.3%), <3 $\log_{10}$ and ≥2 $\log_{10}$ in 52 patients (25.1%), <2 $\log_{10}$ and ≥1 $\log_{10}$ in 23 patients (11.1%), and <1 $\log_{10}$ in 15 patients (7.3%). Figure 1A shows the rate of a sustained virologic response according to the reduction in HCV RNA levels at 4 weeks after starting therapy in patients with the TT genotype. The rates were higher significantly in patients who achieved a rapid virologic response or had a ≥3 $\log_{10}$ decrease in

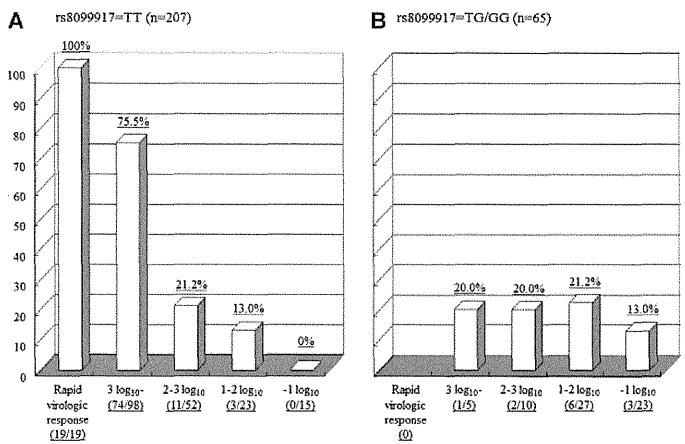

Fig. 1. The rate of sustained virologic responses (%) based on the reduction in serum HCV RNA levels at 4 weeks after starting therapy. **A**: Patients with the TT genotype for rs8099917, (**B**) patients with the TG/GG genotype for rs8099917.

serum HCV RNA levels at 4 weeks compared to those with a <3 $\log_{10}$ decrease in serum HCV RNA levels ($P < 0.0001$). When a 3 $\log_{10}$ decrease in serum HCV RNA levels was defined as the cut-off point, 56.5% of patients were considered to have a ≥3 $\log_{10}$ decrease in serum HCV RNA levels. The sensitivity, specificity, positive predictive value, and negative predictive value for a sustained virologic response were 86.8, 75.2, 78.6, and 84.4%, respectively.

Among the 65 patients who had the TG/GG genotype, no patient achieved a rapid virologic response at 4 weeks after initiating therapy. The decrease in serum HCV RNA levels at 4 weeks after starting therapy ranged from 0.11 $\log_{10}$ to 4.75 $\log_{10}$ (mean, 1.66 $\log_{10}$). The reduction in serum HCV RNA levels at 4 weeks after starting the therapy were smaller in patients with the TG/GG genotype than those with the TT genotype (1.66 ± 1.02 $\log_{10}$ in patients with the TG/GG genotype vs. 3.12 ± 1.37 $\log_{10}$ in patients with TT genotype excluding RVR, $P < 0.0001$). The reduction in serum HCV RNA levels was ≥3 $\log_{10}$ in five patients (7.7%), <3 $\log_{10}$ and ≥2 $\log_{10}$ in 10 patients (15.4%), <2 $\log_{10}$ and ≥1 $\log_{10}$ in 27 patients (41.5%), and <1 $\log_{10}$ in 23 patients (35.4%). Figure 1B shows the rates of a sustained virologic response according to the reduction in HCV RNA levels at 4 weeks after starting therapy in patients with the TG/GG genotype. There were no differences in the rate of a sustained virologic response based on the reduction in HCV RNA levels at 4 weeks after starting therapy; the rate of a sustained virologic response remained at 20% approximately regardless of the reduction in HCV RNA levels in 42 patients with a ≥1 $\log_{10}$ reduction in serum HCV RNA levels.

Association Between an Early Virologic Response at 12 Weeks and Treatment Outcome Based on Genetic Polymorphisms Near the *IL28B* Gene

Figure 2 shows the rate of patients with the TT genotype or TG/GG genotype for rs8099917 who achieved a complete early virologic response, a partial early virologic response, and those who did not achieve early virologic response at 12 weeks after starting therapy based on the reduction in serum HCV RNA level at 4 weeks after initiating therapy. Nearly 75% of patients with the TT genotype whose HCV RNA levels were reduced by ≥3 $\log_{10}$ at 4 weeks after starting the therapy achieved a complete early virologic response. In contrast, 80% of patients with the TG/GG genotype whose HCV RNA levels were reduced by ≥3 $\log_{10}$ at 4 weeks after starting the therapy showed a partial early virologic response. The majority of patients with the TT or TG/GG genotypes achieved a partial early virologic response when their reduction in HCV RNA levels was <3 $\log_{10}$ and ≥2 $\log_{10}$ or <2 $\log_{10}$ and ≥1 $\log_{10}$.

Figure 3 shows the rates of a sustained virologic response according to the type of early virologic response in patients with the TT genotype (Fig. 3A) and TG/GG genotype (Fig. 3B). Among patients with the TT genotype, the rate of sustained virologic response was significantly higher in patients with a complete early virologic response than in those with a partial early virologic response ($P < 0.0001$). In contrast, there was no difference in the rate of a sustained virologic response between patients with a complete early virologic response and those with a partial early virologic response ($P = 0.8917$) among patients with

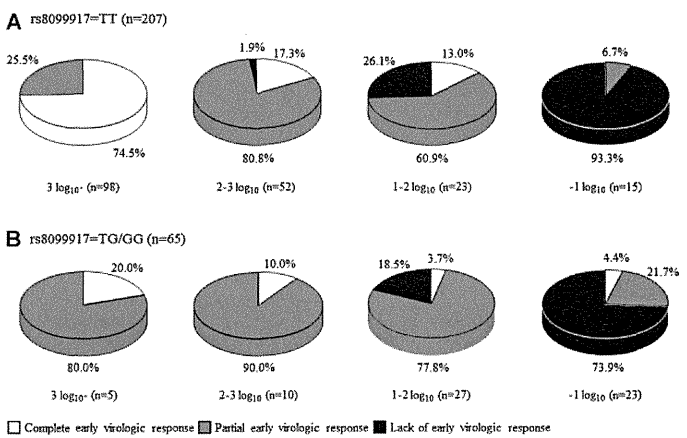

Fig. 2. The association between the virologic responses at 12 weeks after starting therapy and the reduction in serum HCV RNA levels at 4 weeks after starting therapy. **A**: Patients with the TT genotype for rs8099917, (**B**) patients with the TG/GG genotype for rs8099917.

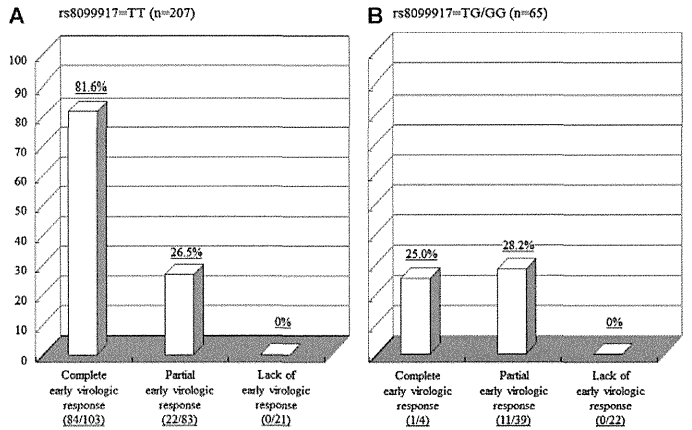

Fig. 3. The rate of sustained virologic responses based on the type of early virologic response. **A**: Patients with the TT genotype for rs8099917, (**B**) patients with the TG/GG genotype for rs8099917.

the TG/GG genotype. None of the patients with the TT genotype or TG/GG genotype who yielded a lack of an early virologic response reached a sustained virologic response.

Univariate and Multivariate Analyses for Factors Associated With a Sustained Virologic Response to Peginterferon and Ribavirin Combination Therapy in Patients With the TT and the TG/GG Genotype for the rs8099917

Univariate and multivariate analyses were conducted for factors associated with a sustained virologic response based on different genetic polymorphisms near the *IL28B* gene. In patients with the TT genotype, the factors that were associated with a sustained virologic response included serum alkaline phosphatase levels, serum albumin, platelet counts, hepatitis activity grade, liver fibrosis grade, reduction in HCV RNA levels at 4 weeks after starting therapy, and a complete early virologic response based on a univariate analysis (Table IIIA). In a multivariate analysis, the serum albumin levels, reduction in HCV RNA levels 4 weeks after starting therapy, and a complete early virologic response were independent factors that were significantly associated with a sustained virologic response (Table IIIB). A reduction in HCV RNA levels 4 weeks after starting therapy was the strongest factor that affected a sustained virologic response. In patients with the TG/GG genotype, the factors that were associated with a sustained virologic response included patient age, platelet counts, and pretreatment HCV RNA levels based on a univariate analysis (Table IIIA). A reduction in the HCV RNA levels at 4 weeks after starting therapy was not associated with a sustained virologic response. In a multivariate analysis, patient age and pretreatment HCV RNA levels were independent factors that were significantly associated with a sustained virologic response (Table IIIC).

Characteristics of Patients who Achieved a Sustained Virologic Response to the Combination Therapy Despite the Unfavorable TG/GG Genotype Near the *IL28B* Gene

Table IV shows the characteristics of 12 patients who achieved a sustained virologic response despite having the unfavorable TG/GG genotype for rs8099917 near the *IL28B* gene. All but one patient was under 60 years old and had liver fibrosis not more than grade 2 (one patient did not undergo a liver biopsy). Except for one patient, the reduction in the serum HCV RNA levels at 4 weeks after starting therapy was less than 3 $\log_{10}$ and all but one patient showed a partial early virologic response at 12 weeks after starting the therapy. In all 11 patients with a partial early virologic response, the serum HCV RNA was undetectable up to 24 weeks after starting the therapy. All but one patient extended the treatment duration from 48 to 72 weeks (two patients discontinued therapy at 60 weeks during the extended treatment period). When the characteristics of patients who achieved a sustained virologic response were compared between those with the unfavorable TG/GG genotype and those with the favorable TT genotype, patients with the TG/GG genotype were younger (41.8 ± 14.4 years vs. 55.1 ± 10.4 years, $P = 0.0023$) and had lower pretreatment HCV RNA levels (5.91 ± 0.44 $\log_{10}$ IU/ml vs. 6.21 ± 1.05 $\log_{10}$ IU/ml, $P = 0.0199$).

TABLE III. Univariate and Multivariate Analyses for Factors Associated With a Sustained Virologic Response to Peginterferon and Ribavirin Combination Therapy in Patients With the TT and the TG/GG Genotype for the rs8099917

(A) Univariate analyses	*P*-value	
	Patients with TT genotype of rs8099917 (n = 207)	Patients with TG/GG genotype of rs8099917 (n = 65)
Age (years)	0.0505	0.0007
Sex (female/male)	0.1830	0.2296
Body weight (kg)	0.6891	0.2456
Alanine aminotransferase (IU/L)	0.7988	0.4032
Aspartate aminotransferase (IU/L)	0.5021	0.1705
Gamma-glutamyl transpeptidase (IU)	0.6340	0.6648
Alkaline phosphatase (IU/L)	0.0315	0.0599
Albumin (g/dl)	0.0002	0.6594
Total bilirubin (mg/dl)	0.2929	0.7130
White blood cell count (/μl)	0.2508	0.5549
Hemoglobin (g/dl)	0.0847	0.2289
Platelet count ($\times 10^3$/μl)	0.0454	0.0411
Liver histology-activity (A0–1/A2–3)	0.0445	0.1117
Liver histology-fibrosis (F0–1/F2–3)	0.0002	0.2283
Pretreatment HCV RNA concentration ($\geq$6.5 $\log_{10}$ vs. <6.5 $\log_{10}$)	0.5279	0.0379
Reduction in the peginterferon dose	0.4316	0.5563
Reduction in the ribavirin dose	0.1823	0.4272
Reduction in HCV RNA levels at 4 weeks after starting the therapy ($\geq$3 $\log_{10}$ vs. < 3 $\log_{10}$)	<0.0001	0.9265
Early virologic response (complete vs. partial)	<0.0001	0.9777
Early virologic response (partial vs. non)	0.8632	0.0686

(B) Multivariate analyses: Patients with TT genotype of rs8099917	*P*-value	Odds ratio (95% confidence interval)
Alkaline phosphatase (IU/L)	0.2617	
Albumin (g/dl)	0.0365	28.287 (1.4107–755.41)
Platelet count ($\times 10^3$/μl)	0.2599	
Liver histology-activity (A0–1/A2–3)	0.6678	
Liver histology-fibrosis (F0–1/F2–3)	0.2307	
Reduction in HCV RNA levels at 4 weeks after starting the therapy ($\geq$3 $\log_{10}$ vs. <3 $\log_{10}$)	<0.0001	16.029 (6.8593–40.406)
Early virologic response (complete vs. partial)	0.0224	0.3685 (0.1557–0.8749)

(C) Multivariate analyses: Patients with TG/GG genotype of rs8099917	*P*-value	Odds ratio (95% confidence interval)
Age (years)	0.0022	0.0034 (0.0000–0.0840)
Platelet count ($\times 10^3$/μl)	0.3344	
Pretreatment HCV RNA concentration ($\geq$6.5 $\log_{10}$ vs. <6.5 $\log_{10}$)	0.0304	0.0548 (0.0020–0.4950)

HCV, hepatitis C virus.

DISCUSSION

Several previous studies reported that patients who achieved a rapid virologic response, in which serum HCV RNA become undetectable at 4 weeks after starting therapy, had a high likelihood of achieving a sustained virologic response [Martinez-Bauer et al., 2006; Poordad et al., 2008; de Segadas-Soares et al., 2009; Martinot-Peignoux et al., 2009]. In addition, several recent studies reported the predictive value of the degree of reduction in serum HCV RNA levels at 4 weeks after starting therapy [Yu et al., 2007; Huang et al., 2010; Toyoda et al., 2011]. Therefore, the viral dynamics of HCV at 4 as well as 12 weeks after starting therapy is important for response-guided therapy.

Genetic polymorphisms near the *IL28B* gene have emerged as the strongest predictive factor of a sustained virologic response in patients infected with HCV genotype 1 [Hayes et al., 2011; Kurosaki et al., 2011]. In addition, Thompson et al. [2010 reported that genetic polymorphisms near the *IL28B* gene were associated strongly with early viral dynamics during PEG-IFN and ribavirin combination therapy. These findings raised an important issue of whether response-guided therapy, based on the reduction in serum HCV RNA levels at 4 or 12 weeks after starting

TABLE IV. Patients who Achieved a Sustained Virologic Response Despite the TG/GG Genotype for the rs8099917

	Age (years)	Sex	Liver histology	Pretreatment HCV RNA level (log_{10} IU/ml)	HCV RNA reduction at 4 weeks	Response at 12 weeks	HCV RNA became undetectable (weeks)	Treatment duration (weeks)
1.	31	Female	A1/F1	6.13	2.19	partial EVR	20	48
2.	55	Male	A1/F1	5.80	1.77	partial EVR	16	72
3.	57	Female	A1/F1	5.58	3.01	partial EVR	16	72
4.	57	Female	A1/F1	6.21	1.81	partial EVR	20	72
5.	62	Male	N.D.	6.23	1.13	partial EVR	24	72
6.	21	Male	A1/F2	6.04	1.83	partial EVR	24	72
7.	42	Male	A1/F1	6.27	0.57	partial EVR	24	72
8.	29	Female	A1/F2	5.83	1.83	partial EVR	20	60
9.	52	Male	A1/F0	5.91	2.12	complete EVR	12	48
10.	40	Male	A2/F1	5.84	1.34	partial EVR	20	72
11.	27	Male	N.D.	5.63	0.42	partial EVR	24	72
12.	28	Male	A1/F0	6.59	0.76	partial EVR	20	60

N.D., not done; HCV, hepatitis C virus; EVR, early virologic response.

therapy, retains a predictive value when considering genetic polymorphisms near the *IL28B* gene.

In the present study, the predictive value of the decrease in serum HCV RNA levels was evaluated at 4 and 12 weeks after starting therapy in Japanese patients infected with HCV genotype 1b based on genetic polymorphisms near the *IL28B* gene. Consistent with previous reports, patients with the TG/GG genotype for rs8099917 had a smaller reduction in serum HCV RNA levels at 4 weeks after starting treatment ($P < 0.0001$), which indicates an unfavorable response to the combination therapy. Patients with the TT genotype for rs8099917, which is associated with a favorable response to the combination therapy, exhibited a significant difference in the rate of a sustained virologic response based on the reduction in serum HCV RNA levels at 4 weeks after initiating the therapy. Patients with a rapid virologic response or with a ≥ 3 log_{10} reduction in HCV RNA levels had a higher likelihood of achieving a sustained virologic response.

In contrast, these factors did not have any predictive value in patients with the TG/GG genotype. Only 18.5% of patients achieved a sustained virologic response (12 of 65 patients), and it was difficult to identify these patients based on the reduction in HCV RNA levels at 4 weeks or the type of an early virologic response at 12 weeks after starting therapy. Patients who achieved a sustained virologic response, despite the TG/GG genotype for rs8099917, were identified among those with a <2 log_{10} and ≥ 1 log_{10} or even <1 log_{10} reduction in HCV RNA levels at 4 weeks after starting therapy. Interestingly and paradoxically, the possibility of a sustained virologic response can be expected in patients with a <1 log_{10} reduction in HCV RNA levels at 4 weeks after starting therapy only when they have the unfavorable TG/GG genotype.

In the evaluation at 12 weeks after starting therapy, patients with the TT genotype who achieved a complete early virologic response had a higher rate of a sustained virologic response significantly than patients who achieved a partial early virologic response, whereas this difference was not found in patients with the TG/GG genotype. No patients who failed to achieve an early virologic response achieved a sustained virologic response regardless of the genetic polymorphisms near the *IL28B* gene. Thus, the lack of an early virologic response retained a strong predictive value for the failure of achieving a sustained virologic response. This result supports the recommendation in the AASLD guidelines, in which treatment may be discontinued in patients without an early virologic response at 12 weeks of treatment.

The characteristics of patients who achieved a sustained virologic response despite the unfavorable TG/GG genotype were younger in age and lower pretreatment HCV RNA levels. Most patients with the TG/GG genotype who achieved a sustained virologic response showed a partial early virologic response and extended the treatment duration. It was difficult to identify these patients according to viral dynamics at 4 or 12 weeks after starting therapy.

There are several limitations in this study. Some patients with a slow virologic response did not have their treatment period extended from 48 to 72 weeks. This is because the effectiveness of a 72-week combination therapy regimen in patients with HCV genotype 1 with a slow virologic response [Berg et al., 2006; Pearlman et al., 2007] had not been established in Japan in the earlier part of this study. This fact might have influenced the treatment outcome especially in patients with the unfavorable TG/GG genotype. Another limitation is a smaller sample size of patients with the TG/GG genotype in comparison to that of patients with the TT genotype. This sample size could have caused the lack of statistical significance in the rate of a sustained virologic response according to the reduction in HCV RNA levels at 4 weeks after starting therapy or according to the type of an early virologic response in patients with the TG/GG genotype. In addition, the data were based on Japanese patients infected with HCV genotype 1b. Therefore, these results should be confirmed in other ethnicities and patients infected with HCV genotype 1a.

In conclusion, among patients infected with HCV genotype 1b with the TT genotype for rs8099917, a rapid virologic response or a ≥ 3 log_{10} reduction in HCV RNA levels at 4 weeks after starting therapy, or a complete early virologic response indicate strongly that these patients will achieve a sustained virologic response as a final outcome for PEG-IFN and ribavirin combination therapy. Early viral dynamics retain the predictive value in this patient subpopulation. A reduction in HCV RNA levels at 4 weeks after starting therapy or the type of an early virologic response does not predict the likelihood that patients with the TG/GG genotype will achieve a sustained virologic response. In contrast, the lack of an early virologic response retains a strong predictive value for the failure to achieve a sustained virologic response regardless of *IL28B* polymorphisms, which remains useful as a factor to stop therapy.

REFERENCES

Abe H, Ochi H, Maekawa T, Hayes CN, Tsuge M, Miki D, Mitsui F, Hiraga N, Imamura M, Takahashi S, Ohishi W, Arihiro K, Kubo M, Nakamura Y, Chayama K. 2010. Common variation of *IL28B* affects gamma-GTP levels and inflammation of the liver in chronically infected hepatitis C virus patients. J Hepatol 53:439–443.

Berg T, Sarrazin C, Herrmann E, Hinrichsen H, Gerlach T, Zachoval R, Wiedenmann B, Hopf U, Zeuzem S. 2003. Prediction of treatment outcome in patients with chronic hepatitis C: Significance of baseline parameters and viral dynamics during therapy. Hepatology 37:600–609.

Berg T, von Wagner M, Nasser S, Sarrazin C, Heintges T, Gerlach T, Buggisch P, Goeser T, Rasenack J, Pape GR, Schmidt WE, Kallinowski B, Klinker H, Spengler U, Martus P, Alshuth U, Zeuzem S. 2006. Extended treatment duration for hepatitis C virus type 1: Comparing 48 versus 72 weeks of peginterferon-alfa-2a plus ribavirin. Gastroenterology 130:1086–1097.

Buti M, Sanchez-Avila F, Lurie Y, Stalgis C, Valdes A, Martell M, Esteban R. 2002. Viral kinetics in genotype 1 chronic hepatitis C patients during therapy with 2 different doses of peginterferon alfa-2b plus ribavirin. Hepatology 35:930–936.

Colucci G, Ferguson J, Harkleroad C, Lee S, Romo D, Soviero S, Thompson J, Velez M, Wang A, Miyahara Y, Young S, Sarrazin C. 2007. Improved COBAS TaqMan hepatitis C virus test (version 2.0) for use with the High Pure system: Enhanced genotype inclusivity and performance characteristics in a multisite study. J Clin Microbiol 45:3595–3600.

Davis GL, Wong JB, McHutchison JG, Manns MP, Harvey J, Albrecht J. 2003. Early virologic response to treatment with peginterferon alfa-2b plus ribavirin in patients with chronic hepatitis C. Hepatology 38:645–652.

de Segadas-Soares JA, Villela-Nogueira CA, Perez RM, Nabuco LC, Brandao-Mello CE, Coelho HSM. 2009. Is the rapid virologic response a positive predictive factor of sustained virologic response in all pretreatment status genotype 1 hepatitis C patients treated with peginterferon-α2b and ribavirin? J Clin Gastroenterol 43:362–366.

Fried MW, Shiffman ML, Reddy KR, Smith C, Marinos G, Goncales FL Jr, Haussinger D, Diago M, Carosi G, Dhumeaux D, Craxi A, Lin A, Hoffman J, Yu J. 2002. Peginterferon alfa-2a plus ribavirin for chronic hepatitis C virus infection. N Engl J Med 345: 975–982.

Ge D, Fellay J, Thompson AJ, Simon JS, Shianna KV, Urban TJ, Heinzen EL, Qiu P, Bertelsen AH, Muir AJ, Sulkowski M, McHutchison JG, Goldstein DB. 2009. Genetic variation in *IL28B* predicts hepatitis C treatment-induced viral clearance. Nature 461:399–401.

Ghany MG, Strader DB, Thomas DL, Seeff LB. 2009. Diagnosis, management, and treatment of hepatitis C: An update. Hepatology 49:1335–1374.

Hayes NC, Kobayashi M, Akuta N, Suzuki F, Kumada H, Abe H, Miki D, Imamura M, Ochi H, Kamatani N, Nakamura Y, Chayama K. 2011. HCV substitutions and *IL28B* polymorphisms on outcome of peg-interferon plus ribavirin combination therapy. Gut 60:261–267.

Huang C-F, Yang J-F, Huang J-F, Dai C-Y, Chiu C-F, Hou N-J, Hsieh M-Y, Lin Z-Y, Chen S-C, Hsieh M-Y, Wang L-Y, Chang W-Y, Chuang W-L, Yu M-L. 2010. Early identification of achieving a sustained virological response in chronic hepatitis C patients without a rapid virological response. J Gastroenterol Hepatol 25:758–765.

Kurosaki M, Tanaka Y, Nishida N, Sakamoto N, Enomoto N, Honda M, Sugiyama M, Matsuura K, Sugauchi F, Asahina Y, Nakagawa M, Watanabe M, Sakamoto M, Maekawa S, Sasaki A, Kaneko S, Ito K, Masaki N, Tokunaga K, Izumi N, Mizokami M. 2011. Pretreatment prediction of response to pegylated-interferon plus ribavirin for chronic hepatitis C using genetic polymorphism in *IL28B* and viral factors. J Hepatol 54:439–448.

Lee SS, Ferenci P. 2008. Optimizing outcomes in patients with hepatitis C virus genotype 1 or 4. Antiviral Ther 13:S9–S16.

Marcellin P, Rizzetto M. 2008. Response-guided therapy: Optimizing treatment now and in the future. Antiviral Ther 13:S1–S2.

Martinez-Bauer E, Crespo J, Romero-Gomez M, Moreno-Otero R, Sola R, Tesei N, Pons F, Forns X, Sanchez-Tapias JM. 2006. Development and validation of two models for early prediction of response to therapy in genotype 1 chronic hepatitis C. Hepatology 43:72–80.

Martinot-Peignoux M, Maylin S, Moucari R, Ripault M-P, Boyer N, Cardoso A-C, Giuily M, Castelnau C, Pouteau M, Stern C, Auperin A, Bedossa P, Asselah T, Marcellin P. 2009. Virological response at 4 weeks to predict outcome of hepatitis C treatment with pegylated interferon and ribavirin. Antivir Ther 14:501–511.

McCarthy JJ, Li JH, Thompson A, Suchindran S, Lao XQ, Patel K, Tillmann HL, Muir AJ, McHutchison JG. 2010. Replicated association between an *IL28B* gene variant and a sustained response to pegylated interferon and ribavirin. Gastroenterology 138:2307–2314.

Pearlman BL, Ehleben C, Saifee S. 2007. Treatment extension to 72 weeks of peginterferon and ribavirin in hepatitis C genotype 1-infected slow responders. Hepatology 46:1688–1694.

Pittaluga F, Allice T, Abate ML, Ciancio A, Cerutti F, Varetto S, Colucci G, Smedile A, Ghisetti V. 2008. Clinical evaluation of the COBAS Ampliprep/COBAS TaqMan for HCV RNA quantitation in comparison with the brancd-DNA assay. J Med Virol 80:254–260.

Poordad F, Reddy KR, Martin P. 2008. Rapid virologic response: A new milestone in the management of chronic hepatitis C. Clin Infect Dis 46:78–84.

Rauch A, Kutalik Z, Descombes P, Cai T, Di Iulio J, Mueller T, Bochud M, Battegay M, Bernasconi E, Borovicka J, Colombo S, Cerny A, Dufour JF, Furrer H, Günthard HF, Heim M, Hirschel B, Malinverni R, Moradpour D, Müllhaupt B, Witteck A, Beckmann JS, Berg T, Bergmann S, Negro F, Telenti A, Bochud PY. Swiss Hepatitis C Cohort Study; Swiss HIV Cohort Study. 2010. Genetic variation in *IL28B* is associated with chronic hepatitis C and treatment failure: A genome-wide association study. Gastroenterology 138:1338–1345.

Suppiah V, Moldovan M, Ahlenstiel G, Berg T, Weltman M, Abate ML, Bassendine M, Spengler U, Dore GJ, Powell E, Riordan S, Sheridan D, Smedile A, Fragomeli V, Müller T, Bahlo M, Stewart GJ, Booth DR, George J. 2009. *IL28B* is associated with response to chronic hepatitis C interferon-alpha and ribavirin therapy. Nat Genet 41:1100–1104.

Tanaka Y, Nishida N, Sugiyama M, Kurosaki M, Matsuura K, Sakamoto N, Nakagawa M, Korenaga M, Hino K, Hige S, Ito Y, Mita E, Tanaka E, Mochida S, Murawaki Y, Honda M, Sakai A, Hiasa Y, Nishiguchi S, Koike A, Sakaida I, Imamura M, Ito K, Yano K, Masaki N, Sugauchi F, Izumi N, Tokunaga K, Mizokami M. 2009. Genome-wide association of *IL28B* with response to pegylated interferon-alpha and ribavirin therapy for chronic hepatitis C. Nat Genet 41:1105–1109.

The French METAVIR Cooperative Study Group. 1994. Intraobserver and interobserver variations in liver biopsy interpretation in patients with chronic hepatitis C. Hepatology 20:15–20.

Thompson AJ, Muir AJ, Sulkowski MS, Ge D, Fellay J, Shianna KV, Urban T, Afdhal NH, Jacobson IM, Esteban R, Poordad F,

Lawitz EJ, McCone J, Shiffman ML, Galler GW, Lee WM, Reindollar R, King JW, Kwo PY, Ghalib RH, Freilich B, Nyberg LM, Zeuzem S, Poynard T, Vock DM, Pieper KS, Patel K, Tillmann HL, Noviello S, Koury K, Pedicone LD, Brass CA, Albrecht JK, Goldstein DB, McHutchison JG. 2010. Interleukin-28B polymorphism improves viral kinetics and is the strongest pretreatment predictor of sustained virologic response in genotype 1 hepatitis C virus. Gastroenterology 139: 120–129.

Toyoda H, Kumada T, Kiriyama S, Tanikawa M, Hisanaga Y, Kanamori A, Tada T, Arakawa T, Fujimori M, Niinomi T, Ando N, Yasuda S, Sakai K, Kimura J. 2011. High ability to predict the treatment outcome of peginterferon and ribavirin combination therapy based on the reduction in HCV RNA levels at 4 weeks after starting therapy and amino acid substitutions in hepatitis C virus in patients infected with HCV genotype 1b J Gastroenterol 46:501–509.

Yu JW, Wang GQ, Sun LJ, Li XG, Li SC. 2007. Predictive value of rapid virological response and early virological response on sustained virological response in HCV patients treated with pegylated interferon α-2a and ribavirin. J Gastroenterol Hepatol 22:832–836.

Zeuzem S, Herrmann E, Lee JH, Fricke J, Neumann AU, Modi M, Colucci G, Roth WK. 2001. Viral kinetics in patients with chronic hepatitis C treated with standard or peginterferon alpha2a. Gastroenterology 120:1438–1447.

Research Article

EASL EUROPEAN ASSOCIATION FOR THE STUDY OF THE LIVER | JOURNAL OF HEPATOLOGY

p53/p66Shc-mediated signaling contributes to the progression of non-alcoholic steatohepatitis in humans and mice

Kengo Tomita[1,2,*,†], Toshiaki Teratani[2,†], Takahiro Suzuki[2], Tetsuya Oshikawa[2], Hirokazu Yokoyama[3], Katsuyoshi Shimamura[2], Kiyoshi Nishiyama[4], Norikazu Mataki[1], Rie Irie[5], Tohru Minamino[6], Yoshikiyo Okada[1], Chie Kurihara[1], Hirotoshi Ebinuma[2], Hidetsugu Saito[7], Ippei Shimizu[6], Yohko Yoshida[6], Ryota Hokari[1], Kazuo Sugiyama[2], Kazuo Hatsuse[4], Junji Yamamoto[4], Takanori Kanai[2], Soichiro Miura[1], Toshifumi Hibi[2]

[1]*Division of Gastroenterology and Hepatology, Department of Internal Medicine, National Defense Medical College, 3-2 Namiki, Tokorozawa-shi, Saitama 359-8513, Japan;* [2]*Division of Gastroenterology and Hepatology, Department of Internal Medicine, Keio University School of Medicine, 35 Shinanomachi, Shinjuku-ku, Tokyo 160-8582, Japan;* [3]*Health Center, Keio University School of Medicine, 35 Shinanomachi, Shinjuku-ku, Tokyo 160-8582, Japan;* [4]*Department of Surgery, National Defense Medical College, 3-2 Namiki, Tokorozawa-shi, Saitama 359-8513, Japan;* [5]*Department of Pathology, Kawasaki Municipal Hospital, 12-1 Shinkawadori, Kawasaki-ku, Kawasaki-shi, Kanagawa 210-0013, Japan;* [6]*Department of Cardiovascular Science and Medicine, Chiba University Graduate School of Medicine, 1-8-1 Inohana, Chuo-ku, Chiba 260-8670, Japan;* [7]*Graduate School of Pharmaceutical Sciences, Keio University Faculty of Pharmacy, 1-5-30 Shibakoen, Minato-ku, Tokyo 105-8512, Japan*

Background & Aims: The tumor suppressor p53 is a primary sensor of stressful stimuli, controlling a number of biologic processes. The aim of our study was to examine the roles of p53 in non-alcoholic steatohepatitis (NASH).

Methods: Male wild type and p53-deficient mice were fed a methionine- and choline-deficient diet for 8 weeks to induce nutritional steatohepatitis. mRNA expression profiles in normal liver samples and liver samples from patients with non-alcoholic liver disease (NAFLD) were also evaluated.

Results: Hepatic p53 and p66Shc signaling was enhanced in the mouse NASH model. p53 deficiency suppressed the enhanced p66Shc signaling, decreased hepatic lipid peroxidation and the number of apoptotic hepatocytes, and ameliorated progression of nutritional steatohepatitis. In primary cultured hepatocytes, transforming growth factor (TGF)-β treatment increased p53 and p66Shc signaling, leading to exaggerated reactive oxygen species (ROS) accumulation and apoptosis. Deficient p53 signaling inhibited TGF-β-induced p66Shc signaling, ROS accumulation, and hepatocyte apoptosis. Furthermore, expression levels of p53, p21, and p66Shc were significantly elevated in human NAFLD liver samples, compared with results obtained with normal liver samples. Among NAFLD patients, those with NASH had significantly higher hepatic expression levels of p53, p21, and p66Shc compared with the group with simple steatosis. A significant correlation between expression levels of p53 and p66Shc was observed.

Conclusions: p53 in hepatocytes regulates steatohepatitis progression by controlling p66Shc signaling, ROS levels, and apoptosis, all of which may be regulated by TGF-β. Moreover, p53/p66Shc signaling in the liver appears to be a promising target for the treatment of NASH.

Keywords: P53; Non-alcoholic steatohepatitis; P66Shc; Reactive oxygen species; Transforming growth factor-β.

Received 9 December 2011; received in revised form 14 May 2012; accepted 21 May 2012; available online 26 May 2012

* Corresponding author. Address: Division of Gastroenterology and Hepatology, Department of Internal Medicine, National Defense Medical College, 3-2 Namiki, Tokorozawa-shi, Saitama 359-8513, Japan. Tel.: +81 4 2995 1211x2369; fax: +81 4 2996 5201.

E-mail address: kengo@ndmc.ac.jp (K. Tomita).

† These authors contributed equally to this work.

Abbreviations: NAFLD, non-alcoholic fatty liver disease; NASH, non-alcoholic steatohepatitis; ROS, reactive oxygen species; MCD, methionine-deficient and choline-deficient; ALT, alanine aminotransferase; HE, haematoxylin-eosin; HNE, hydroxynonenal; TUNEL, terminal deoxy-nucleotidyl transferase-mediated nick end-labeling; PCR, polymerase chain reaction; TGF-β, transforming growth factor-β; PFT, pifithrin; Col11, 1 (I) collagen; Col12, 2 (I) collagen; SMA, smooth muscle actin; MDA, malondialdehyde.

Introduction

Non-alcoholic fatty liver disease (NAFLD) afflicts as much as 20% of the US adult population [1]. Non-alcoholic steatohepatitis (NASH)—part of the spectrum of NAFLD—is the most prevalent liver disease in the US, affecting approximately 3–4% of the population [1].

NAFLD and NASH are often co-morbid with disorders characterized by insulin resistance, such as diabetes and obesity. Thus, these liver diseases can be considered hepatic manifestations of metabolic syndrome. Given the growing number of patients with metabolic syndrome, the incidences of NAFLD and NASH are expected to increase further, particularly in North America, Europe, Asia, and countries in the Western Pacific.

NASH is a progressive disease. In a study that followed NASH patients for ten years, the disease progressed to cirrhosis in 20% of the patients and led to fatal liver disease in 8% of the cases [2]. A population-based cohort study demonstrated that

ELSEVIER

Journal of Hepatology **2012** vol. 57 | 837–843

Table 1. Histological characteristics of patients.

	NASH (n = 57)	Simple steatosis (n = 13)
Steatosis		
1	31	10
2	18	3
3	8	0
Inflammatory activity		
0	0	11
1	9	2
2	43	0
3	5	0
Fibrosis stage		
0	0	13
1	35	0
2	14	0
3	8	0
4	0	0

approximately 3% of the patients diagnosed with NAFLD developed cirrhosis or a liver-related complication [3]. The progressive nature and serious consequences of NASH highlight the need for effective therapies. The pathologic mechanisms underlying NASH, however, have not yet been clarified.

Recently, a number of diagnostic tests that incorporate clinical markers, including age, have been reported for NAFLD. Indeed, advanced age is a major risk factor for the progression of NASH [4]. On the other hand, the tumor suppressor p53—a master sensor of stressful conditions—controls many biological processes, including aging [5]. Reactive oxygen species (ROS), which are thought to make major contributions to aging, stimulate p53 stabilization and subsequent induction of apoptosis via a feed-forward regulatory loop [6]. Hepatic p53 expression is elevated in patients with NASH [7]. A recent report has also shown that hepatic p53 expression and hepatocyte apoptosis significantly increase in a mouse model of NASH [8]. These results suggest that p53 plays a role in the pathophysiology of NASH.

In the present study, we examined the role of p53 signaling during NASH using p53-deficient mice and a mouse model of NASH. We found that hepatic p53 signaling markedly contributes to the pathogenesis of NASH. Our findings suggest hepatic p53 signaling as a promising target for new modalities in the treatment of NASH.

Materials and methods

Please refer to the Supplementary Materials and methods section for more detailed descriptions.

Animal studies

Eight-week-old male C57BL/6J mice were purchased from CLEA Japan Inc. $p53^{+/-}$ mice were purchased from Jackson Laboratories (Bar Harbor, Maine, USA). $p53^{+/+}$ and $p53^{-/-}$ mouse littermates were obtained from crosses of $p53^{+/-}$ mice with the C57BL/6J background.

In experiments for nutritional steatohepatitis, 8-week-old male $p53^{+/+}$ mice or $p53^{-/-}$ mouse littermates were fed a methionine- and choline-deficient (MCD) diet (cat No. 960439; ICN, Aurora, Ohio) or a standard chow (CE-2; CLEA Japan Inc.) for 8 weeks. In order to make a time-course analysis of nutritional steatohepatitis, 8-week-old male C57BL/6J mice were fed an MCD diet for 3 or 8 weeks.

All animals received humane care in compliance with the National Research Council's criteria outlined in the "Guide for the Care and Use of Laboratory Animals", prepared by the US National Academy of Sciences and published by the US National Institutes of Health.

Human liver tissue samples

Liver tissues were obtained from 70 patients undergoing ultrasound-guided liver biopsy for suspected NASH and from 10 patients undergoing surgical operation at the Keio University School of Medicine and National Defense Medical College. Patient characteristics are shown in Table 1. Written informed consent was obtained from all patients. This study protocol was approved by the Ethical Committee of the Keio University Hospital and National Defense Medical College Hospital, and followed the ethical guidelines of the Declaration of Helsinki.

Statistical analysis

Data are expressed as means (SEM) or median and interquartile range. Statistical analyses were performed using unpaired Student's *t* test, one-way analysis of variance (ANOVA), or Mann–Whitney's U test for univariate comparison, as appropriate. Correlations were assessed using the Pearson product-moment correlation coefficient. Differences were considered statistically significant at p values less than 0.05. All of the computations were performed with a commercial statistical package (SPSS version 12, Chicago, USA).

Results

p53 deficiency ameliorates the progression of nutritional steatohepatitis in mice

Following administration of an MCD diet, mice rapidly and consistently develop a severe form of steatohepatitis with the characteristic pathology of steatosis, mixed cell inflammatory infiltrate, hepatocyte death, and pericellular fibrosis, which resembles human NASH [9]. Therefore, to examine the effects of p53 signaling on the progression of NASH, we fed wild type and p53-deficient mice an MCD diet for 8 weeks. After 8 weeks of MCD diet, the p53-deficient mice exhibited significantly fewer lipid droplets in their hepatocytes, and reduced infiltration of inflammatory cells into their livers, compared with those observed in the wild type group (Fig. 1A). The MCD diet also produced a higher increase of serum alanine aminotransferase (ALT) levels in wild type mice than in p53-deficient mice (Fig. 1B). After 8 weeks of MCD diet, the livers of wild type mice exhibited a significant increase in lipid droplets in hepatocytes and elevated hepatic TG concentrations compared with p53-deficient mice (Fig. 1C).

Moreover, the livers of wild type mice showed increased collagen deposition, whereas fibrosis was markedly reduced in the livers of p53-deficient mice (Fig. 1A). Quantification of Masson trichrome staining and liver hydroxyproline levels confirmed the histologic results (Fig. 1D). Those levels were significantly lower in p53-deficient mice compared with wild type mice (Fig. 1D). Real-time PCR analyses of whole liver homogenates from mice fed the MCD diet revealed significantly increased mRNA levels of collagen type 1 α1 (*Col1α1*), collagen type 1 α2 (*Col1α2*), and transforming growth factor *(TGF)-β*, compared with those of mice fed the control diet. Compared with the wild type livers, the livers of p53-deficient mice showed significantly decreased mRNA expression of *Col1α1*, *Col1α2*, and *TGF-β* after the mice were fed the MCD diet (Fig. 1E). The MCD diet significantly increased hepatic mRNA expression of α-*SMA* (smooth muscle actin), a marker of hepatic stellate cell activation; p53-deficient mice showed significantly lower levels of expression compared to wild type mice (Fig. 1E).

p53 signaling regulates hepatic ROS accumulation in nutritional steatohepatitis

Hepatic ROS accumulation is thought to play a role in the pathogenesis of NASH [10–12]. We immunostained samples for 4-hydroxynonenal (4-HNE) protein adducts as products of lipid peroxidation. Lipid peroxidation in the liver was significantly enhanced in mice with nutritional steatohepatitis compared with mice fed the control diet (Fig. 1F). Compared with p53-deficient mice, wild type mice showed more intense staining of hepatocytes after being fed the MCD diet (Fig. 1F). Levels of malondialdehyde (MDA)—another product of lipid peroxidation—in liver homogenates also showed that inhibition of p53 signaling significantly decreased hepatic lipid peroxidation in nutritional steatohepatitis (Fig. 1G).

p53 deficiency decreases hepatocyte susceptibility to damage in a mouse model of nutritional steatohepatitis

Because liver injury in NASH is associated with increased hepatocyte apoptosis [10], we performed terminal deoxynucleotidyl transferase-mediated nick end-labeling (TUNEL) assays to evaluate apoptosis in mice with nutritional steatohepatitis. The percentage of TUNEL-positive apoptotic hepatocytes was significantly larger in the group fed the MCD diet than in the group fed the control diet, while p53 deficiency significantly ameliorated this effect (Fig. 1H and I).

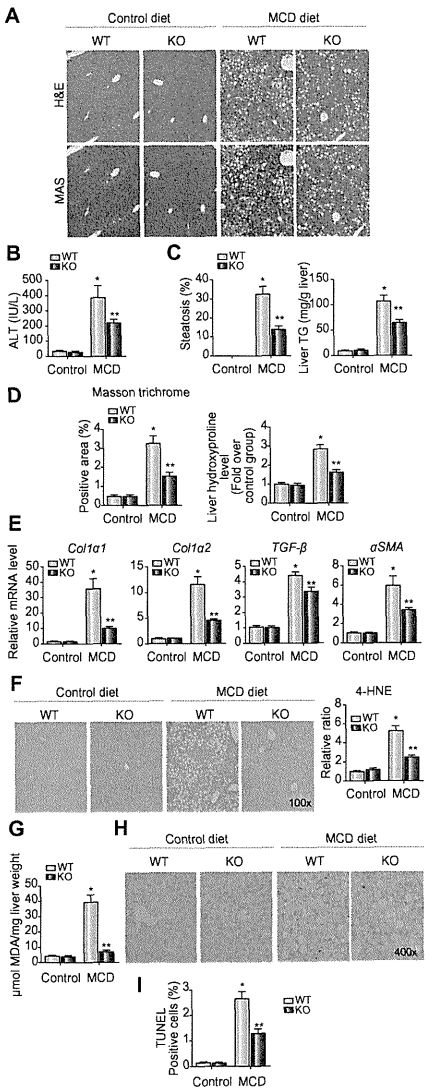

Fig. 1. Effect of p53 deficiency on nutritional steatohepatitis, ROS accumulation, and hepatocyte injury, induced by MCD dietary feeding. (A) Effect of hepatic p53 deficiency on nutritional steatohepatitis. Haematoxylin-eosin (H&E)-stained and Masson trichrome-stained sections of liver samples are representative of the indicated groups, which received the MCD or control diet for 8 weeks (magnification, 100×). (B) Serum ALT activity in the indicated groups. (C) The percentage of hepatocytes involved in steatosis (left) and hepatic TG levels (right). (D) Quantification of Masson trichrome staining (left) and liver hydroxyproline concentrations (right). Values are means ± SEM (n = 6–9 mice/group). KO, p53-deficient mice; WT, wild type mice. *p <0.05 compared with wild type mice fed the control diet. **p <0.05 compared with wild type mice fed the MCD diet. (E) Real-time PCR analysis was used to quantitate hepatic mRNA levels of *Col1α1*, *Col1α2*, *TGF-β*, and α-*SMA* (n = 6–9 mice/group). *p <0.05 compared with wild type mice fed the control diet. **p <0.05 compared with wild type mice fed the MCD diet. (F) The effect of p53 deficiency on 4-HNE expression. Representative 4-HNE-stained sections (left). Quantification of 4-HNE staining (right). (G) Liver MDA levels in the indicated groups. Values are means ± SEM (n = 5 mice/group). *p <0.05 compared with wild type mice fed the control diet. **p <0.05 compared with wild type mice fed the MCD diet. (H) The effect of p53 deficiency on hepatocyte apoptosis. Representative TUNEL-stained sections. (I) Percentages of TUNEL-positive hepatocytes (n = 6–8 mice/group). *p <0.05 compared with wild type mice fed the control diet, and **p <0.05 compared with wild type mice fed the MCD diet. (This figures appears in color on the web).